DESIGN AND DEVELOPMENT OF DIODE PUMP FIBRE LASER TURNING SET UP

By

AYAN SAHA

Bachelor of Engineering in Production Engineering, 2014
Jadavpur University
Kolkata

Examination Roll No.   M4PRD1607
Registration No.   112088 of 2010-2011

THESIS
SUBMITTED IN PARTIAL FULFILMENT OF THE REQUIREMENTS FOR THE AWARD OF THE DEGREE OF MASTER OF PRODUCTION ENGINEERING IN THE FACULTY OF ENGINEERING & TECHNOLOGY, JADAVPUR UNIVERSITY
2016

DEPARTMENT OF PRODUCTION ENGINEERING
JADAVPUR UNIVERSITY
KOLKATA-700032
INDIA

FACULTY OF ENGINEERING AND TECHNOLOGY
JADAVPUR UNIVERSITY
KOLKATA

Date:

Certificate of Recommendation

I HEREBY RECOMMEND THAT THE THESIS ENTITLED **"DESIGN AND DEVELOPMENT OF DIODE PUMP FIBRE LASER TURNING SET UP"** CARRIED OUT UNDER MY SUPERVISION AND GUIDANCE BY **AYAN SAHA** MAY BE ACCEPTED IN THE PARTIAL FULLFILLMENT OF THE REQUIREMENTS FOR THE DEGREE OF **"MASTER OF PRODUCTION ENGINEERING".**

—————————————————————

Prof. Soumya Sarkar
Thesis Advisor
Department of Production Engineering
Jadavpur University
Kolkata-700032

——————————————————   ——————————————————

Prof. Debmalya Banerjee   **Prof. Sivaji Bandyopadhyay**
Head of the Department   **Dean**
Department of Production Engineering   **Faculty of Engg & Tech**
Jadavpur University   **Jadavpur University**
Kolkata-700032   **Kolkata-700032**

FACULTY OF ENGINEERING AND TECHNOLOGY
JADAVPUR UNIVERSITY
KOLKATA

*Certificate of Approval**

The foregoing thesis is hereby approved as a creditable study of an engineering subject carried out and presented in a manner of satisfactory to warrant its acceptance as a pre-requisite to the degree for which it has been submitted. It is understood that by this approval, the undersigned do not necessarily endorse or approve any statement made, opinion expressed and conclusion drawn therein but approve the thesis only for the purpose for which it has been submitted.

COMMITEE ON FINAL EXAMINATION FOR EVALUATION OF THE THESIS

EXTERNAL EXAMINER

INTERNAL EXAMINER

* Only in case the recommendation is concurred in.

DECLEARATION OF ORIGINALITY AND COMPLIANCE OF ACADEMIC ETHICS

I, hereby declare that this thesis contains literature survey and original research work by the undersigned candidate, as part of his Master of Production Engineering studies.

All information in this document have been obtained and presented in accordance with academic rules and ethical conduct.

I also declare that, as required by rules and conduct, I have fulfilled cited and referenced all material and results that are not original to this work.

THESIS TITLE: "DESIGN AND DEVELOPMENT OF DIODE PUMP FIBRE LASER SET-UP"

CANDIDATE NAME: AYAN SAHA

EXAMINATION ROLL NO: M4PRD16907

UNIVERSITY REGISTRATION NO: 112088 of 2010-2011

_____

Signature with Date

Acknowledgement

This thesis is outcome of the efforts of several personalities with whom I worked during this tenure. First of all I want to acknowledge the inspiration and help provided by my honourable project advisors Dr. Soumya Sarkar (Professor, Department of Production Engineering, J.U.) & Dr. Debmalya Banerjee (Head of the Department, Department of Production Engineering, J.U.), without whom, this project was not possible. His efforts and motivation always remained my constant source of inspiration.

I express deep respect to all the faculty members of the department for their inspiration and help during the entire period of this thesis work.

I also owe a gratitude for all laboratory and academic staff for their valuable time and suggestions.

I am also thankful to the Librarian and research scholars of Production Engineering Department, Jadavpur University for their cordial assistance.

I thankfully acknowledge the support of all those people, who some time or the other directly or indirectly rendered their help at different stages of this work.

Finally I bow to my parents, my all-family member, well-wisher for their blessing and inspiration without which it was next to impossible to achieve my goal.

<div align="right">

(AYAN SAHA)

</div>

TABLE OF CONTENTS

Chapter-1

1. INTRODUCTION

Laser beam machining (LBM) is a non-traditional subtractive manufacturing process, a form of machining, in which a laser is directed towards the work piece for machining. This process uses thermal energy to remove material from metallic or non-metallic surfaces. The laser is focused onto the surface to be worked and the thermal energy of the laser is transferred to the surface, heating and melting or vaporizing the material. Laser beam machining is best suited for brittle materials with low conductivity, but can be used on most materials.

Lasers can be used for welding, cladding, marking, surface treatment, drilling, and cutting among other manufacturing processes. It is used in the automobile, shipbuilding, aerospace, steel, electronics, and medical industries for precision machining of complex parts. Laser welding is advantageous in that it can weld at speeds of up to 100 mm/s as well as the ability to weld dissimilar metals. Laser cladding is used to coat cheep or weak parts with a harder material in order to improve the surface quality. Drilling and cutting with lasers is advantageous in that there is little to no wear on the cutting tool as there is no contact to cause damage. Milling with a laser is a three dimensional process that requires two lasers, but drastically cuts costs of machining parts. Lasers can be used to change the surface properties of a work piece.

Laser beam machining can also be used in conjunction with traditional machining methods. By focusing the laser ahead of a cutting tool the material to be cut will be softened and made easier to remove, reducing cost of production and wear on the tool while increasing tool life.

The appliance of laser beam machining varies depending on the industry. In heavy manufacturing laser beam machining is used for cladding and drilling, spot and seam welding among others. In light manufacturing the machine is used to engrave and to drill other metals. In the electronic industry laser beam machining is used for wire stripping and skiving of circuits. In the medical industry it is used for cosmetic surgery and hair removal.

1.1 NEED OF THE PRESENT RESEARCH

- Small components free of micro-cracks, good edge and surface quality as well as with a high aspect ratio, made of hard materials such as ceramics and glass, HSTR alloys, MMC etc are difficult to fabricate and often require complex, multi-step processing.

- High demands for micro features (like groove, step turned surface, holes etc) in these materials have been increasing for a number of miniature product applications such as in MEMS device packaging, optical fibre alignment, mini-vision systems and microelectronic packaging.

- Sometimes three dimensional surface-texturing of hard to machine pure metals and alloys using pulsed laser system is a new direction in the area of laser micro machining. This cannot be achieved by any other NTM process.

- Ceramics materials which are unable to machine by EDM/WEDM, ECM can be easily fabricated by laser machining process and we can generate intricate shapes and miniaturised parts on these materials.

- Direct write laser processing, in which the material removal occurs at high power densities during the laser ablation process, has been regarded as a powerful technique. Compared to other conventional and non conventional techniques of machining, laser machining offers a number of advantages such as single-step processing, high flexibility, direct writing of features by integrating CAD/CAM software. Precise focusing of the laser beam allows material removal with high accuracy, high repeatability and localized material removal with micron size tolerances. A relative comparison of micro machining techniques is given below in the table1

Machining process	Capital investment	Tooling or Fixtures	Power requirements	Removal efficiency	Tool wear
Conventional machining	Low	Low	Low	Very low	Low
Ultrasonic machining	Low	Low	Low	High	Medium
Electrochemical machining	Very high	Medium	Medium	Low	Very low
Chemical machining	Medium	Low	High	Medium	Very low
Electro-discharge machining	Medium	High	Low	High	High
Plasma-arc machining	Very low	Low	Very low	Very low	Very low
Laser machining	Medium	Low	Very low	Very high	Very low

TABLE1: Relative comparisons of different NTM processes

1.2 FUNDAMENTALS OF LBM PROCESS

Laser beam machining (LBMM) is a thermal energy based advanced machining process in which the material is removed by (i) Melting, (ii) Vaporization, and (iii) Ablation (bonds are broken which causes the materials to degrade). When a high energy density laser bream is focused on work surface the thermal energy is absorbed which heats and transforms the work volume into a molten or vaporized state that can easily be removed by flow of high-pressure assist gas jet (which accelerates the transformed material and ejects it from machining zone).
In this process a beam of highly coherent light called a Laser is directed towards the work piece for machining. Since the rays of a laser beam are monochromatic and parallel it can be focused to a very small diameter and can produce power density as high as 100 MW for a square millimetre of area. It is especially suited to make accurately placed holes. It can be used to perform precision micro-machining on all microelectronic substrates such as ceramic, silicon, diamond, and graphite. The term "light" is generally accepted to be electromagnetic radiation ranging from 1 nm to 1000 mm in wavelength. The visible spectrum (what we see) ranges from approximately 400 to 700 nm. The wavelength range from 700 nm to 10 mm is considered the near infrared (NIR), and anything beyond that is the far infrared (FIR). Conversely, 200 to 400 nm is called ultraviolet (UV); below 200 nm is the deep ultraviolet (DUV).

The light generated by stimulated emission is very similar to the input signal in terms of wavelength, phase, and polarization. This gives laser light its characteristic coherence, and allows it to maintain the uniform polarization and often monochromaticity established by the optical cavity design.

Material removal mechanism

The basic material removal mechanism involved in laser beam machining is dependent upon the generation of high heat flux that causes melting and vaporization of the material where the beam is focused. A suitable lasing medium is used to get the laser beam of suitable wavelength. Fig 1.1 shows the working of a laser. The beam coming out of a lasing medium has a small diameter. The beam is then focused on the material surface using a good focusing lens. Laser beam has a well-defined wave front, which is either plane or spherical. When such a beam passes through a lens, the beam should get focused to a point. As a result, a high-energy concentration is obtained at that point. The laser radiation is first absorbed by the material surface where the optical energy is converted into heat.

The amount of absorption of laser radiation by a work piece mainly depends on the wavelength, the angle of incidence of the laser beam on the work piece as well as polarization and finally the intensity of the focused laser beam. This intense heat melts and vaporizes the material.
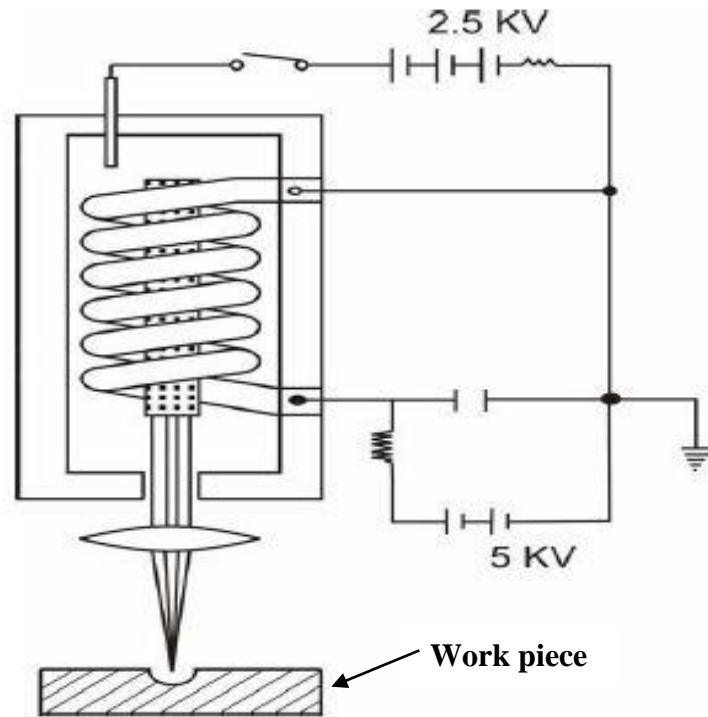
FIG. Working of a laser

The excitation energy provided by the laser is rapidly converted into heat and this is followed by various heat transfer processes such as conduction into the materials, convection and radiation from the surface. The temperature distribution within the material as a result of these heat transfer processes depends on the thermo physical properties of the material (density, emissivity, thermal conductivity, specific heat, thermal diffusivity), dimensions of sample (thickness) and laser processing parameters (absorbed energy, beam cross-sectional area). The magnitude of temperature rise due to heating governs the different physical effects in the material such as

(a) Melting and sublimation

(b) Vaporization and dissociation

(c) Plasma formation

(d) Ablation

Which are responsible for micro material removal / machining.

Melting & sublimation

At high laser power densities the surface temperature of the material may reach the melting point and material removal takes place by melting. The surface temperature increases with increasing irradiation time, reaches maximum temperature T_{max} at laser ON-time and then decreases.

The solid–liquid interface can be predicted by tracking the melting point in temperature versus depth Before initialization of surface evaporation, maximum melt depth increases with laser power density I (power per unit area) at constant pulse time while at a constant laser power density, maximum depth of melting increases with increasing pulse time. Prediction of melt depth using temperature profiles assists in determining depth of machined cavity in those glasses in which material removal takes place entirely or in part by melting.

Vaporization & dissociation

As the surface temperature of material reaches the boiling point, further increase in laser power density or pulse time removes the material by evaporation instead of melting. After vaporization starts at the material surface, the liquid–vapour interface moves further inside the material with supply of laser energy and material is removed by evaporation from the surface above the liquid–vapour interface. Several works in the past have considered material removal only through this direct evaporation mechanism. In such cases, the depth of evaporation corresponding to depth of machined cavity depends on the laser conditions (processing time and absorbed laser energy) and material properties such as density, latent heat of vaporization, and boiling point during machining process and dissociation energy losses also affect the input laser energy and thus the temperature distribution, dimensions of machined cavity and machining time. The total enthalpy required for laser-induced vaporization being greater than that required for melting, the energy required for laser machining by melting is much less than the energy required for machining by vaporization. It was reported that a combination of the different physical phenomena mentioned above was responsible for machining rather than any single predominant process.

Plasma formation

When the laser energy density surpasses a certain threshold limit, the material immediately vaporizes, gets ionized and forms plasma having temperatures as high as 50,000°C and pressures up to 500MPa.The plasma plume forms a shield over the machining area and reduces the energy available to the work piece when the surface temperature exceeds a certain threshold value. Aerosols formed due to the condensation of ionized material vapour stick to the surface and reduces the efficiency of machined components for applications dominated by wear or tear load. Hence the degree of ionization is an important parameter which gives an indication whether plasma will be formed during the machining process and accordingly, necessary efforts to overcome the harmful effects of plasma could be undertaken. A special gas nozzle designed prevents the deposition of aerosols and this technique has been successfully applied to machine material surfaces without any debris. The additional gas stream obtained by combining a process gas stream and an exhaust stream transports the vaporized material and avoids radial distribution of the plasma.

Continuous application of laser pulses ensures that each successive spot is adequately displaced to reduce the plasma absorption effects. Furthermore, short duration pulses reduce the recast layer thickness; eliminate micro-cracks and the material removed per pulse increases with increasing energy density while machining ceramic materials.

Ablation

When the material is exposed to sufficiently large incident laser energy, the temperature of the surface exceeds the boiling point of the material causing rapid vaporization and subsequent material removal by the process referred to as thermal ablation. Ablation takes place when laser energy exceeds the characteristic threshold laser energy which represents the minimum energy required to remove material by ablation. Above ablation threshold energy, material removal is facilitated by bond breaking, whereas thermal effects take place below ablation threshold energy. Absorption properties of the glass and incident laser parameters determine the location at which the absorbed energy reaches the ablation threshold.

The sharp focusing of a laser light with sufficient fluencies is an attractive tool for material ablation. The type of interaction between the laser light and the material depends on laser parameters (wavelength, pulse duration and fluency) and on the properties (absorption coefficient, energy band gap, melting temperatures, the effective evaporation temperatures, and thermal conductivities) of the material. Ablation process can be categorized into three different mechanisms:

(a) Photo thermal

(b) Photochemical

(c) Photo physical

Photo thermal ablation is a thermal ablation process, in which instantaneous transformation of excitation energy into heat causes the removal of material. The rapid dissipation of the excitation and ionization energy from the electrons to the lattice, the material surface is heated rapidly and vaporized explosively with or without surface melting. These results in relatively high ablation rates and a rough surface finish. At moderate to high fluencies of nanosecond-pulsed lasers, screening of the incident radiation by vapour/plasma plume becomes significant. The screening effect would diminish laser light intensity that reaches the substrate by absorption and scattering within the vapour plume. Additionally, with decreasing wavelength of laser light, laser–plasma interaction becomes less pronounced

If the photon energy of the laser light is sufficiently high, the probability of non-linear absorption increases strongly and multi-photon absorption is favoured. Under these conditions, laser excitation can result in direct bond scission, and the process is called photochemical ablation. For purely photochemical (non-thermal) processes, the temperature of the system remains essentially unchanged under laser irradiation. The ablation rate is relatively slow ($\leq 1\mu m$/pulse), but high surface quality can be achieved. It is also called as photolytic processes. In photolytic processes the photon energy is directly applied to overcome the chemical bonding energy of (macro) molecules. When all laser energy is used to overcome the chemical binding energy, the ideal case, it is known as "cold ablation".

Photo physical includes both thermal and non-thermal mechanisms contributing to overall ablation processes. In the laser ablation process, significant ablation is observed only above a certain laser fluence, which is referred as the threshold fluence. The values of the threshold fluence depend on laser parameters, in particular laser wavelength and pulse duration.

1.3 LASER MICROMACHINING

Lasers are increasingly used for a precise micromachining because of its high flexibility, contactless machining, the ability to machine a large variety of materials including plastics, metals, semiconductors, ceramics and other materials that are difficult to process such as diamond, glass and graphite. The primary mechanisms of material removal during precision micromachining of materials are ablation and etching. The material removal by these mechanisms can be performed in three different ways: direct writing, mask projection technique, interference technique. Some of the process parameters which control the laser micromachining are laser wavelength, beam shape, delivered energy, pulse width, focal length and pulse repetition rate. The beam quality also influences the uniformity in micromachining.

Micro-machining is the basic technology of micro engineering for the production of miniature component. It is a set of processes for creating structures, devices or systems with feature sizes of the order of micrometer. In industry there is a tendency towards miniaturization of products.

Micro-manufacturing is an exciting and emerging area of modern technology because engineering components shrink in size as the technology progresses For example, the feature size of integrated circuit chips has been reduced nearly 20 times over the past three decades. There is growing interest in the precise fabrication of micro- and nanostructures such as motors, optics, sensors, fluid control devices, actuators, miniature valves, pacemakers, Implants, and catheters. The traditional mechanical approaches of cutting, drilling, and shaping materials are no longer satisfactory for fabricating micron scale structures. Instead, beam techniques based on photons, electrons, and ions are used to produce high-resolution structures.

Lasers have been used to solve fine machining problems in numerous fields, including for medical devices, telecommunication, microelectronics, fibre optics, data storage, instrumentation, and micro-optics Lasers have been proven as effective tools in micromachining.

Non–conventional machining is now receiving acknowledgement of its importance because of some of its specific advantages, which can be exploited during the micromachining operation. According to the machining phenomena, the micro machining processes were classified under the following heads: removal by mechanical force, melting and vaporization, ablation, dissolution, plastic deformation, solidification, lamination. Major methods of micro-machining are shown in table 1.1. Though there are various types of micro-machining processes, here micro-cutting, micro drilling, marking and cleaning are discussed later.

1.4 VARIOUS LASER MICRO MACHINING TECHNIQUES

Mask projection technique

The majority of excimer laser systems used in manufacturing applications use the technique of mask projection.
In standard mask projection systems, the depth of the micro-structures is controlled by the numbers of laser shots which are fired and the resolution of the features are determined by the mask and the optical projection system. This is demonstrated in Figure. 1.8 Where micro-channels of 18 μm depth have been produced in a polymer. The entire sample area (which can be many tens or hundreds of centimetre square) is machined under the same laser conditions and so all the micro-structures are produced to the same depth. This is, in fact, highly desirable in most applications since uniformity of depth is of particular importance.

Direct writing technique

The current generation of solid-state lasers (e.g. Nd:YAG, Nd:YVO3, Ti:sapphire) and some gas lasers (e.g. CO2 lasers) offer a large number of attractive benefits for direct writing technique.
In direct write systems, the laser beam is focused to a small spot using a lens and either the beam or the sample (or both) are moved around to produce the desired pattern. In some cases, additional galvanometer-controlled scanning mirrors are also included. If scanning mirrors are used, then a flat-field lens is required as this keeps the focal plane position constant irrespective of the angle of the beam being deflected from the scanning mirrors. Beam spot sizes of a few tens of microns can be easily achieved with such systems and the combination of scanner mirrors and high repetition rate lasers means that very high processing speeds can be achieved.

Using both of these techniques the following machining can be done:

(a) Laser drilling

(b) Laser cutting

(c) Laser Grooving

(d) Laser marking & cleaning

Laser cutting

Mechanical cutting is a method for creating miniature devices and components with features that range from tens of micrometers to a few millimetres in size. Even though the mechanical micro cutting process may not be capable of obtaining the smallest feature sizes used in lithographic processes, mechanical cutting processes are very important in bridging the macro-domain and the nano and micro domains for making functional components. This is especially true for complex microstructures requiring a variety of materials, interfaces and functional shapes to form micro systems that function within the macro-domain. The principle of micro cutting is similar to those of conventional cutting operations.

Advantages of laser cutting over mechanical cutting include easier work holding and reduced contamination of work piece (since there is no cutting edge which can become contaminated by the material or contaminate the material).

Precision may be better, since the laser beam does not wear during the process. There is also a reduced chance of warping the material that is being cut, as laser systems have a small heat affected zone.

The main disadvantage of laser cutting is the high power consumption. Industrial laser efficiency may range from 5% to 15%. The power consumption and efficiency of any particular laser will vary depending on output power and operating parameters. This will depend on type of laser and how well the laser is matched to the work at hand. The amount of laser cutting power required, known as heat input, for a particular job depends on the material type, thickness, process (reactive/inert) used, and desired cutting rate.

Laser drilling

Laser drilling operation can be used to produce micro-hole in almost any material. Holes less than 0.25mm in diameter are difficult to drill mechanically, laser drilling offers an excellent alternative for small hole drilling, especially for hard and brittle materials, such as ceramics and gemstones. Large holes can be drilled by trepanning, i.e., by overlapping and drilling the circumference of a circle to form a large hole.

High throughput of hole drilling are realized by mask projection and automation. Laser hole drilling in materials such as ceramics, copper, nickel, brass, aluminium, borosilicate glass, quartz, rubber and composite materials offer high accuracy for the medical device industry, semiconductor manufacturing and nanotechnology support systems. Laser drilling provides consistency for manufacturing specifications relying on tight tolerances for high depth-to diameter ratios. Laser drilled hole sizes vary depending on laser power, motion control and galvo systems. Laser drilling can provide dynamic, "on-the-fly "changing of hole diameter, hole depth and edge quality.

Laser grooving

During laser grooving, a laser beam is scanned over the work piece surface, resulting in increasing its temperature above the material's melting point, in a small region near the beam spot. In cases where the heat flux, provided by the process parameters, is enough, vaporization of the material might also occur. A gas jet is applied coaxially or off-axially along with the laser beam in order to remove the molten material and produce the groove. Laser grooving is used in various manufacturing applications, such as the creation of micro channels for cooling systems and the creation of slots for assembly.

Laser marking

Laser marking provides a unique combination of speed, permanence and versatility. This technology can generate considerable savings in reduced manufacturing and tooling costs,

elimination of secondary processes and consumable material, and reduced inventory and maintenance downtime. The technique has been used extensively in the production of indelible and legible alpha-numeric characters and logos for product identification and traceability in the semiconductor industry.

Laser marking is essentially a thermal process that employs a high intensity beam of focused laser light to create a contrasting mark on the material surface. Beam-steered marking employs mirrors mounted on high-speed, computer-controlled galvanometers to direct the laser beam across the target surface.

Laser turning

In laser turning process a proper dimension of beam of a laser light is focused to a rotating work piece at any cylindrical surface and the job is fed to the rotating direction. There are several advantages of using high intense laser beam as tool material over conventional micro-turning process. These include elimination of excessive wear of the cutting tool, no surface defects and cracks, ability of machining materials irrespective of hardness or brittleness, no deflection and vibration of machine-tool etc.

Laser cleaning

Laser technologies have demonstrated very promising application for restoration purpose in art conservation. Laser cleaning of stone, metals, painting, paper etc. The origin of this success is the high control of the deteriorated material removal achieved by exploiting case by case the intrinsic characteristics of laser ablation. Laser cleaning is a good candidate for this task. The most important characteristics are:-

Laser cleaning is essentially a surface treatment, where only a thin layers limited to a few microns or less than a micron is directly involve by absorption of light, while chemical method usually perfuse with solvents internal layers without control.

The ablation threshold of high absorption materials (black encrustation for example) is lower than low absorption material (light colour stone for example), so that a selective removal is possible without problems to preserve historical layers.

Laser micromachining has played a significant role in manufacturing of MEMS devices, optical switches and micro motors etc. There is no doubt micro manufacturing combined with micro-engineering will be a key technology in coming years.

1.5 ADVANTAGES OF LASER BEAM MACHINING

Application involving the use of fibre laser to have increased significantly in the last several years. This is largely due to several characteristics of laser machining and the advantages they offer when compared to other micro machining methods as listed. Setup time can be substantially reduced; laser micro-machining layout can be easily created in CAD programs for efficient production of new designs. Laser micro-machining uses lamp-pumped lasers; diode lasers or fibre lasers and has distinct advantages over other micro-machining methods. The advantages of laser micro-machining are given as follows:

    (i)   High quality machining:

Laser systems produce precise micro-cracks free, good edge and surface quality product making this technique very suitable for a wide range of products. This inherently accurate technique produces reproducible high definition artefact.

    (ii)   Greater design flexibility:

Laser machining offers more flexibility of design than is possible with other methods. As there is no direct contact with the surface to be machined, the laser equipment can create profiles of geometrically complex, uneven or otherwise in accessible surfaces. Even more design flexibility is possible because the controlling software enables rapid change of multiple profiles. Small batches and prototypes can be produced more easily thus reducing the overall time to market considerably.

    (iii)   Low operating cost:

By using laser machining technology, today's MEMS manufacturers can realize substantial cost savings when compared to other micro-grooving technologies. With the advances in ultra shot laser pulses and different harmonics of diode pumped solid state laser, laser micro-machining has become an attractive alternative to conventional techniques. In this world of just-in-time manufacturing, laser micro-machining gives the panel manufacturer the advantage they need remain competitive in this demanding field.

    (iv)   Non-contact and automated process:

Laser machining is a noncontact process; therefore no tools wear is encountered. Moreover it does not add excessive heat to the product and generates no physical deformation or chemical change to the product. Laser micro-machining can easily access small indented areas that conventional techniques cannot touch. It can be easily integrated into automated production lines hence involving no additional handling. Laser micro-machining can be applied to products with various geometries and can be optimally computer controlled. Micro-machined can be changed quickly by computer without re-tooling. Rejection rates are low so the laser micro-machining equipment can be safely integrated into the assembly line.

1.6 APPLICATIONS OF LASER BEAM MACHINING

Laser beam machining is now receiving acknowledgement of its importance because of some of its specific advantages, which can be exploited during the micromachining operation. Since lasers can be used in wide range of manufacturing applications such as:

- Material removal- micro drilling, cutting and trepanning
- Welding
- Cladding
- Alloying

Lasers are used not only in manufacturing processes but also in various other fields such as:

- Medicine- Bloodless surgery, laser healing, surgical treatment, eye treatment.
- Defence- Marking targets, alternative to radar, blinding troops.
- Fingerprint detection in the forensic identification.

1.7 SAFETY MEASURES TO BE TAKEN DURING LASER MACHINING

Some of the safety measures that are to be taken while operating the laser machine to prevent the operator and the machine from getting affected are mentioned below:

1. Always use approved and insulated tools when working on HV cables.
2. Always stop the laser with solid absorbent.
3. Never use inflammable objects in the path of the beam.
4. Reflective components incorrectly angled relative to the user (operator) position should be avoided.
5. During the laser operation the person in working area must wear suitable protective goggles.
6. Beware of high voltage electrical equipments.
7. Due to risk of laser radiations never aim the laser beam at people.
8. Do not allow non intended or unnecessary components to intercept the beam.
9. Always clamp the work piece properly.
10. Do not leave anything other than work piece on the worktable.
11. Do not leave anything on the bellows.
12. Preventive maintenance should be performed regularly based on time and operating hours.
13. Check the optical components for contamination or damage and the cooling system for leaks.
14. Make sure temperature is set properly.
15. Check the DI water in the water tanks of heat exchanger units and the chiller unit.
16. Clean the gut side surface of the machine daily before starting.
17. Clean the focusing lens with tissue paper and acetone daily
18. Replace DI water every month because the conductivity of used DI water is been changed.

1.8 PAST RESEARCH WORKS ON FIBER LASER

Reviews on optimization

Arindam Ghosal & Alakesh Manna [1] investigated results on machining of Al/Al2O3-MMC by ytterbium fiber laser. The effects of the different parameters on the response characteristics are explained. A comprehensive mathematical models for correlating the interactive and higher-order influences of various machining parameters such as laser power, modulation frequency, gas pressure, wait time, pulse width on the machining performance criteria e.g. ,metal removal rate and tapering phenomena has been developed for achieving controlled over fiber laser machining process. The response surface methodology (RSM) is employed to achieve optimum responses i.e., minimum tapering and maximum material removal rate. The parameters wait time and modulation frequency are identified as the most significant and significant parameters for MRR. Modulation frequency range from 600 to 680 Hz taper is minimum. The optimal parametric combination for maximized MRR and minimized taper is identified as 473.12W laser power, 604.54 Hz modulation frequency, 0.18s wait time, 19.82bar assist gas pressure and 93.47% of duty cycle pulse width and finally confirmation tests are conducted to validate the developed models.

Fallah, Corbin & Khajepour [2] used fiber laser to modify the surface composition of a Ti–6Al–4V plate through deposition of the blown powder mixture of Ti–45 wt.%Nb. Scanning electron microscopy and energy dispersive spectroscopy (EDS) were employed to examine the clad sections microstructure and chemical composition. The optimized set of laser processing parameters, including the laser power of 1100 W, the laser scan speed of 350mm/min (or ~5.83 mm/s), the laser spot diameter of 2mm and the powder feed rate of 0.1 g/s was found with the identification of combined parameters, the laser specific energy, the powder density and the newly defined laser supplied energy (i.e. representing the amount of energy given to the unit mass of the blown powder). It is shown that, with these parameters, continuous beads can be formed with pore-free sections and a homogeneous composition corresponding to that of ˘ (Ti, Nb) solid solution phase. Furthermore, Al and V elements are thoroughly replaced with a more biocompatible element, Nb, in the second layer of a Ti–Nb cladding build-up on the surface of the Ti–6Al–4V plate (i.e. after ~1mm in clad thickness from the clad/substrate interface).

Zhang, Li, Liu, Wang & Wang [3] utilized high power picoseconds laser to drill micro-holes in C/SiC composites, and the effects of different processing parameters including the helical line width and spacing, machining time and scanning speed were discussed. To characterize the qualities of machined holes, scanning electron microscope(SEM) was used to analyze the surface morphology, energy dispersive spectroscopy (EDS) and X-ray photoelectric spectroscopy (XPS) were employed to describe the element composition change between the untreated and laser-treated area. The experimental results indicated that all parameters mentioned above had remarkable effects on the qualities of micro-holes such as shape and depth. Additionally, the debris consisted of C, Si and O was observed on the machined surface. The Si C bonds of the SiC matrix transformed into Si O bonds after

machined. Furthermore, the physical process responsible for the mechanism of debris formation was discussed as well.

Ghoshal, Manna & Lall [4] presented an experimental study into the influence of machining parameters of Ytterbium fiber laser during drilling of Al-15wt%Al2O3-MMC. The response surface methodology (RSM) is used to achieve optimum responses i.e. minimum tapering and maximum material removal rate (MRR) [1]. A comprehensive mathematical model for correlating the interactive and higher order influences of Ytterbium fiber laser machining parameters such as laser power, modulation frequency, gas pressure, wait time, pulse width on metal removal rate and tapering phenomena has been developed for achieving controlled over fiber laser machining process. Test results reveal that MRR is increased with decrease of wait time and laser power. At wait time 17.5 s and laser power 500 w the MRR is maximum i.e 0.23 g/s. Due to less wait time, the possibility of heat loss is less so MRR increases.

Zhang, Chen, Zhou & Liao [5] conducted deep penetration laser welding of 12 mm thick stainless steel plate using a 10 kW high-power fiber laser. The effect of the processing parameters on the weld bead geometry was examined, and the microstructure and mechanical properties of the optimal joint were investigated. The results show that the focal position is a key parameter in high-power fiber laser welding of thick plates. There is a critical range of welding speed for achieving good full penetration joint. The type of top shielding gas influences the weld depth. The application of a bottom shielding gas improves the stability of the entire welding process and yields good weld appearances at both the top and bottom surfaces. The maximum tensile stress of the joint is 809 MPa. The joint fails at the base metal far from the weld seam with a typical cup–cone-shaped fracture surface. The excellent welding appearance and mechanical properties indicate that high-power fiber laser welding of a 304 stainless steel thick plate is feasible.

Dhupal et al [6] investigates the relationship of processes parameters of pulsed Nd:YAG laser-turning operation for production of micro-groove on cylindrical workpiece of ceramic material. A microprocessor-based work holding device has been developed to provide the rotational motion of cylindrical work pieces for micro-turning operation. Laser turning of micro-grooves on ceramics is highly demanded in the present industry because of its wide and potential uses in various fields such as automobile, aerospace and bio-medical engineering applications, etc. Experiments have been conducted on laser micro-grooving of aluminum oxide (Al_2O_3). The central composite second-order rotatable design (CCD) had been utilized to plan the experiments and response surface methodology was employed for developing empirical models. Analysis on machining characteristics of pulsed Nd:YAG laser micro-grooving operation was made based on the developed models. In this study, lamp current, pulse frequency, pulse width, assist air pressure and cutting speed of work piece are considered as laser machining process parameters. The process performances such as upper deviation (Yuw), lower deviation (Ylw) and depth (Yd) characteristics of laser-turned micro-grooves produced on cylindrical work piece made of Al_2O_3 were evaluated. Analysis of variance (ANOVA) test had also been carried out to check the adequacy of the developed regression empirical models. The observed optimal process parameter settings are lamp current of 22.517 A, pulse frequency of 1.477 kHz, pulse width of 2.394% of duty cycle,

cutting speed of 10.4283 rpm and assist air pressure of 1.3 kgf/cm2 for achieving minimum upper deviation, lower deviation and depth of laser-turned micro-grooves, and finally the results were experimentally verified. From the analysis, it was found that proper control of the process parameters lead to achieve minimum upper deviation, lower deviation and depth of laser-turned microgrooves produced on cylindrical work piece of Al_2O_3.

Reviews on machining conditions

Walter, Rabiey, Warhanek, Jochum & Wegener [6] presents the results of an investigation into the dressing and truing of hybrid bonded (metal vitrified) CBN grinding wheels using a short-pulsed fibre laser. Truing of complex contours on CBN grinding tools with sharp edges (edge radii of less than 20 mm) could be successfully applied, whereas other dressing methods have been neither technically nor economically successful. Sharpening by laser can provide the same wheel surface topography which is conventionally produced by SiC and/or Al2O3 sharpening tools. Grinding characteristics and long-term performance of the laser-profiled tools are discussed.

Cao, Wanjara, Huang, Munro & Nolting [7] investigated that hybrid laser – metal active gas (MAG) arc welding is an emerging joining technology that is very promising for shipbuilding applications. This technique combines the synergistic qualities of the laser and MAG arc welding techniques, which permits a high energy density process with fit-up gap tolerance. As the heat input of hybrid laser – arc welding (HLAW) is greater than in laser welding, but much smaller than in MAG arc welding, a relatively narrow weld and restricted heat affected zone (HAZ) is obtained, which can minimize the residual stress and distortion. Furthermore, adding MAG arc can increase the penetration depth for a given laser power, which can translate to faster welding speeds or fewer number of passes necessary for one-sided welding of thick plates. In this work, a new hybrid fiber laser – arc welding system was successfully applied to fully penetrate 9.3 mm thick butt joints using a single-pass process through optimization of the groove shape, size and processing parameters.

Powell, Al-Mashikhi, Kaplan & Voisey [8] paper presents the results of an experimental and theoretical investigation into the phenomenon of 'striation free cutting', which is a feature of fibre laser/oxygen cutting of thin section mild steel. The paper concludes that the creation of very low roughness edges is related to an optimization of the cut front geometry when the cut front is inclined at angles close to the Brewster angle for the laser– material combination.

Unt, Lappalainen & Salminen [9] focused on the welding of low alloy steels S355 and AH36 in thicknesses 6, 8 and 10 mm in T-joint configuration using either autogeneous laser welding or laser-arc hybrid welding (HLAW) with high power fiber lasers. The aim was to obtain understanding of the factors influencing the size of the fillet and weld geometry through methodologically studying effects of laser power, welding speed, beam alignment relative to surface, air gap, focal point position and order of processes (in case of HLAW) and to get a B quality class welds in all thicknesses after parameter optimization.

Scintilla, Palumbo, Sorgente & Tricarico [10] investigated the effect of laser cutting parameters on the mechanical behaviour of laser butt welded joints whose edges were obtained by laser cutting was investigated. The paper aims to demonstrate that new high power solid-state fiber lasers not only represent a valid and reliable alternative to the most established CO2 and Nd:YAG laser sources, but also allow to obtain cuts having edges well suited for subsequent direct laser welding. First Ti6Al4V 1 mm thick sheets having edges machined by milling were laser welded. Once the optimal welding condition was determined, the mechanical characterization of sheets cut by fiber laser and then laser welded was performed. Comparative strain analysis performed by a digital image correlation technique highlighted the effect of the gap between the sheets resulting from the different cut edge quality. Experimental results showed that the correct selection of laser cutting parameters allows to obtain butt joints characterised by mechanical properties comparable with the ones obtained by milling. Cutting edge quality in the optimal range of gap values allows to obtain the best mechanical performances of the joint.

Seyed Reza Elmi Hosseini et al [11] presented a comparative study on the influence of fiber laser welding (FLW) and CO2 laser welding (CLW) on the weld bead geometry and the microstructure of fusion zone (FZ) of Inconel 617 was investigated. In CLW joints, the weld bead geometry is Y-type shape. In FLW joints, the weld bead geometry transforms from Y-type to I-type with the decrease of the heat input. The minimum heat input required to achieve the full penetration of the weldment in FLW is lower than the CLW. The melting efficiency in FLW is higher than that in CLW. From the top to the root regions, the secondary dendrite arm spacing (SDAS) in fiber laser welded FZ undergoes a smaller change than that in CO2 laser welded FZ. The elements of Ti, Mo, Cr and Co segregate into the interdendritic regions both in FLW and CLW process. The second phases in CLW with the highest input of 360 J/mm are much larger and more than ones in FLW with the highest heat input of 210.5 J/mm.

Tan, He, Gong, Li & Feng [12] Fiber laser-tungsten inert gas (TIG) hybrid welding technique has been developed for lap joining of dissimilar metals AZ31B Mg alloy to pure copper (T2). The influence of laser power on microstructure and mechanical properties of joints was investigated. The results indicated that acceptable joints could be obtained by adjusting the laser power to the range of 2000–3000 W. In particular, at the laser power of 2500W the average tensile shear strength reached a maximum of 45.3 MPa, representing a 57% joint efficiency relative to the Mg sheet. Greater or less than   cause over or under reaction at the interface, which resulted in the poor joint strength. The different morphologies including Mg–Cu eutectic structure, Mg–Cu intermetallic compound and Mg–Al–Cu ternary intermetallic compound were identified at the Mg/Cu interface. All the joints fractured at the Mg/Cu interface. However, the fracture mode was found to differ. For 2500W the surface was characterized by tearing edge, while that with poor joint strength was almost dominated by smooth surface or flat tear pattern.

Wahba, Mizutani & Katayama [13] Argon-rich shielding gas was replaced by 100% CO2gas for cost reduction in fiber laser-GMA hybrid welding of double-side welded T-joints. The welding process using 100% CO2gas was characterized by a large number of

spatters, while the penetration depth of a weld was increased and porosity was reduced. With the objective of obtaining a buried-arc transfer for the reduction of spatter formation, the welding parameters were optimized by observation with a high-speed video camera. Reduced arc voltage, arc leading arrangement and shortened wire extension were necessary to achieve a buried-arc transfer. A significant reduction in spatter generation could only be obtained by the procedure that the relative distances between the two heat sources in the X and Y directions were controlled to produce a proper profile of the arc cavity that could trap any spatters generated. A regulating action of a key hole was observed to remove the disturbances in the melt flows caused by the arc short-circuiting, and high quality joints with good appearances and very few spatters could be produced.

Adelmann & Hellmann [14] presented an experimental results on rapid single mode fiber laser drilling of ceramic substrates. The materials under study are alumina and aluminum nitride with thicknesses ranging from 0.25 mm and1.5 mm. Both the bore diameter and the drilling speed are optimized by varying the laser focus position, laser power, gas pressure and laser modulation scheme, respectively. Within a design of experiment approach we show that the focus position has the highest influence on the bore diameter and highlight the capability to drill sub-50 µm bore diameters with an almost vanishing taper (1.57◦) and good circularity(≤1.07) using modulated single mode fiber lasers. The required drilling time for, e.g. 0.25 mm alumina is as low as 0.1 ms with, in general, longer drilling times for AlN as compared to Al_2O_3. Using a pre-pigmenting technique the splatter after drilling is completely removed in an ultrasonic bath.

Takahashi et al [15] conducted an investigation of carbon fiber reinforced plastic (CFRP) composite processing with a high-power pulsed fiber laser. A CFRP plate was irradiated with laser light from a pulsed fiber laser with an average power of 125 W, a repetition rate of 167 kHz and a pulse width of 10 ns. The wavelength of the laser light was 1064 nm. A galvanometer scanner was used as the processing head for high-speed scanning of the pulsed laser light. A hatching distance was introduced, and the process ingrates were measured according to the parameters of hatching distance and scanning speed. The walls at the grooves irradiated by laser light were observed using scanning electron microscopy (SEM) and cross-sectional profiles of the processed CFRP were measured using confocal laser scanning microscopy (CLSM).The kerf width was measured by optical microscopy observation of the CFRP sample surface processed by laser irradiation. The growth mechanism of the kerf and heat affected zone (HAZ) structures was investigated based on cross-sectional SEM micrographs of the kerfs. The optimal hatching distance for the target groove depth is discussed, together with the importance of the hatching distance for high-speed and high-quality processing of CFRP. The results indicate that adjustment of the hatching distanceand the scanning speed is important for obtaining both good cutting speed and quality.

Meng et al [16] suggested that blind micro-hole array templates were constructed by laser drilling using a 20 W fiber laser on a Ti6Al4V substrate to improve carrying capacity of Ti6Al4V substrate to biomaterials in this study. The influence of laser parameters on the morphology of the blind holes was investigated and the blind micro-hole array templates

were fabricated by the optimized laser parameters. Three typical morphologies were generated through adjusting laser parameters. The type II micro-hole characterized by column-shaped entrance and a hemispherical dome bottom is believed to have a suitable morphology, which was produced by the optimized laser parameters, i.e., defocusing distance 0 mm, laser average power 16 W, laser irradiation time 1 ms and repetition rate 25 kHz. The blind micro-hole templates with different micro-hole density were constructed by the mentioned-above optimized parameters and then the nano-sized hydroxyl apatite (HA) powders were uniformly deposited into the blind micro-hole templates by electro-phoretic deposition. Finally, the dynamic behavior of laser-drilling process was analyzed.

Serbezov et al [17] studied that metal oxide (MOx, M: titanium, magnesium) and Diamond-Like Carbon (DLC) thin films were synthesized by Pulsed Laser Deposition (PLD) at room temperature and low vacuum of 2 Pa for MO_x and vacuum of $4x10^{-3}$ Pa for DLC films. A fiber based Ytterbium (Yb+) laser operating in the nanosecond regime at a repetition rate of 20 kHz was used as an ablation source. Dense and smooth thin films with a thickness from 120 to 360 nm and an area of up to 10 cm2 were deposited on glass and stainless steel substrates at high growth rates up to 2 nm/s for a laser intensity of 10–12 J/cm^2. The thin films synthesis was compared for two fiber laser modes of operation, at a repetition rate of 20 kHz and with an additional modulation at 1 kHz. The morphology, chemical composition and structure of the obtained thin films were evaluated using optical microscopy, Scanning Electron Microscopy (SEM), Energy Dispersive X-ray Spectroscopy (EDX) and Raman spectroscopy. The morphology of the MO_x thin films and the deposition rate strongly depend on the fiber laser mode of operation. Very smooth surfaces were obtained for the metal oxide thin films deposited at lower deposition rates in the modulation mode at 1 kHz. The effect of the substrate on the DLC film structure was studied. The films deposited on dielectric substrates were identified as typical tetrahedral (ta-C) DLC with high sp3 content. DLC films on metal substrates were found typical a-C amorphous carbon films with mixing sp2/sp3 bonds.

Romero, Otero et al [18] presented a method for surface modification of 3D metallic components, to generate micron-sized features to improve drag and surface interaction with viscous fluids. The technique relays in the selective consolidation of pre-placed powder, directly on the surface of the component, to produce micro-cladding tracks under 50 microns in width. A single mode fibre laser is scanned at high speed on the powder to provide the desired geometry. The requirements and limits of the technique are studied, regarding the laser source, optical setup and powder preplacing methodology, as well as practical aspects for its implementation and some applications.

Demir, Maressa & Previtali [19] suggested that textured surfaces exhibit improved properties in terms of tribological, biological, optical, or wetting performance once the texture is opportunely tailored for purpose. Fibre lasers provide a flexible solution for texturing different materials with different surface structures. In this work, the use of a Q-switched fiber laser for surface texturing for tribological, adhesion and biomedical

applications is demonstrated. The required surface pattern of the application is investigated along with the processing conditions to realize the pattern. Results show the adaptability of the *ns* pulsed fibre laser to achieve various patterns with high productivity and industrial robustness.

Stelzer, Mahrle, Wetzig & Beyeran [20] presented experimental study on inert-gas fusion cutting stainless steel with different types of laser are presented. In particular, the cutting capabilities of a fiber and a CO2 laser beam with similar Rayleigh length have been compared as a function of material thickness with respect to achievable maximum cutting speed, cut edge surface roughness and cut kerf geometry. The most interesting finding achieved so far concerns the observation that the cut kerfs are nearly identical in size but differ qualitatively in shape for both laser types.

Reviews on other laser machining parameters

Mohamed Taib et al [21] have been investigated dynamic characteristics of a multi-wavelength Brillouin–Raman fibre laser (MBRFL) assisted by four- wave mixing through the development of Stokes and anti-Stokes lines under different combinations of Brillouin and Raman pump power levels and different Raman pumping schemes inuring cavity. For a Stokes line of order higher than three, the threshold power was less than the saturation power of its last-order Stokes line. By increasing the Brillouin pump power, the nth order anti-Stokes and the (n+4)th order Stokes power levels were unexpectedly increased almost the same before the Stokes line threshold power. It was also found out that the SBS threshold reduction (SBSTR) depended linearly on the gain factor for the 1st and 2nd Stokes lines, as the first set. This relation for the 3rd and 4th Stokes lines as the second set, however, was almost linear with the same slope before SBSTR _6 dB, then, it approached to the linear relation in the first set when the gain factor was increased to 50 dB. Therefore, the threshold power levels of Stokes lines for a given Raman gain can be readily estimated only by knowing the threshold power levels in which there is no Raman amplification.

Feng Xu, Bates & Zak [22] predicted and optimized the contour laser transmission welding (LTW) process, it is important to understand how the laser energy behaves during transmission through the transparent part. In this study, transmission measurements were made on unreinforced and glass-fiber-reinforced amorphous and semi-crystalline thermoplastics at different thicknesses. Using the ratio of transmitted power to laser power, apparent absorption coefficients and apparent reflections were calculated. The results indicate that there is a linear relationship between the glass fiber volume fraction and the apparent absorption coefficient of reinforced polymers; similar effects were also observed for crystallinity. A simple model was developed to estimate apparent absorption coefficient of reinforced polymers as a function of composition. The apparent reflection increased with crystallinity due to increased backscattering. However, for glass-fiber-reinforced polymers, the apparent reflection displayed a more complex behavior.

Pingxue Li et al [23] report on a 980nm passively mode-locking Yb-doped large mode area photonic crystal fiber oscillator with semiconductor saturable absorber mirror (SESAM) and

nonlinear polarization evolution (NPE) technique, simultaneously. The oscillator generates a maximum average output power of 497mW with a repetition rate of 87.37 MHz. Because of the invisible filter effect of NPE mode-locked fiber laser, we achieved an ultra-short pulse width of 1.24ps. The output spectrum of the pulse is centered at 977.7nm with a full width half maximum (FWHM) of 1.90nm and has a characteristic steep spectral edges of dissipative solution. In this paper, the pulse evolution process of 980nm mode-locking fiber laser is simulated and the experimental results are good agreement with the simulation results.

Shien-Kuei Liaw et al [24] proposed a wide-tuning range linear cavity C+L band tunable fiber laser is in this paper. By using 3-point bending device to facilitate wavelength tuning of fiber Bragg gratings (FBGs), a scheme with two parallel strain-tunable FBGs (TFBGs) is demonstrated in L band operation. A large tuning range of over 22.5 nm with 0.1nm precise resolution for each TFBG is obtained. The over lapping tuning range for two TFBGs is from 1564 to 1600.5nm with 2dB power variation. Using 10 M Erbium-doped fiber (EDF) and 100 MW pumping power, the stable lasing output power is measured at 1582.0 nm with threshold pump power and side mode suppression ratio (SMSR) of 10mW and 50dB, respectively. And the measured slope efficiency is 11.5% corresponding to quantum efficiency of12.3%.

Xiao Shen , Hui Zou et al [25] established the improved rate equations with additional leakage losses of signal light for a uniformly side-pumped Yb^{3+}-doped gain-guided and index-antiguided fiber laser . An exact analytical expression of threshold pump power is obtained. Then the effects of Yb3þ concentration, fiber length, core radius and mirror reflectivity on threshold pump power are discussed in detail, separately. The method of designing the fiber parameters is described while maintaining single mode oscillation, such as R1¼1, R2¼0.75, a¼85 μm, L¼10cm, N¼5_1020 cm_3, and threshold power is 6.3W. Compared with end- pumped scheme, the doped concentration and length of the fiber used inside-pumped scheme can be both larger. The analytical solution was easy to calculate and showed distinct results for the optimal design of the fiber laser.

Shijie Fu ,Quan Sheng et al [26] demonstrated experimentally an actively Q-switched all-fiber laser operating at the wavelength of 1920nm, on a readily accessible commercial Tm-doped silica fiber. The Q-switching is achieved by polarization modulation through the stress-induced birefringence using a piezoelectric transducer (PZT) as the Q-switcher. The pulsed fiber laser can be operated with the repetition rates ranging from tens of kilohertz to nearly two hundreds kilohertz with milliwatt average output power.

G.X. Liu, D.J.Feng et al [27] demonstrated an erbium-doped fiber laser that is passively mode locked by a few-layer graphene saturable absorber. Mono layer grapheme was fabricated on copper foil by the chemical vapor deposition method and the corresponding Raman spectroscopy was measured. Few-layer graphene films were transferred to the end surface of fiber connector by the adsorption effect of Vander Waals force to fabricate the saturable absorber. Stable mode-locked pulses at a central wavelength of 1568.1nm were obtained. The repetition rate, maximum average output power, and pulse width were

7.29MHz, 1.68mW, and 58.8ps, respectively. Experimental results illustrate that few-layer grapheme is a promising saturable absorber for mode-locked fiber laser.

S.V. Kuryntsev & A.Kh.Gilmutdinov [28] investigated the effect of heat treatment on the welded joints of steel grade 0.3C–1Cr–1Si produced by 30kW power fiber laser. The speed of the welding process was 20mm/s. Heat treatment was carried out on two levels, quenching with subsequent middle tempering and high tempering. The samples were examined before and after heat treatment, macro-and microstructure were studied using SEM, UTS, three points bent test, micro hardness. The effect of heat treatment was significant: it allowed reduction of the weld hardness of considerably and enhancement of its ductility

Weihua Zhang & Zesheng Ying [29] proposed and demonstrated experimentally a fiber laser sensor for simultaneous measurement of liquid level and temperature. The sensor is based on two taper structures and a fiber Bragg grating (FBG). The two taper structures form a novel fiber interferometer, which is fabricated by cascading two tapers in a section of single-mode fiber (SMF). The FBG and the interferometer serve as the filters of the laser cavity. Corresponding to the two filters, the laser outputs are stable dual-wavelength outputs, which have different characteristics to the liquid level and the temperature. The wavelength produced by the FBG is not sensitive to the liquid level. The temperature sensitivity of the wavelength produced by the FBG is 0.0123nm/°C. The wavelength produced by the interferometer is sensitive to the liquid level and the sensitivity is up to 0.2294nm/mm. The temperature sensitivity of the wavelength produced by the interferometer is 0.0648nm/°C. According to the different spectral responses of the liquid level and the temperature, simultaneous measurement can be realized. Furthermore, the proposed sensor has the advantages of less detection limit (DL), higher resolution and higher sensitivity compared to other optical fiber sensors.

Xudong Hu & Tigang Ning [30] proposed a temperature-dependent high power Yb3+-doped dual-clad fiber lasers model with stimulated Brillouin scattering (SBS). The numerical simulation results show that the temperature distribution, laser power, pump power and Stokes powers propagating along axial positions are obtained after only few iteration times using number sequence transition method based on MATLAB BVP solvers (NSTM-BVPs).Compared the results of the fiber laser model without temperature factor, the SBS threshold powers and corresponding laser output powers at different fiber lengths and core diameters in our fiber laser model are obtained in detail. The effect of temperature factor on the SBS threshold power cannot be negligible for short fiber length less than 15 m. While for long fiber length, the influences of temperature factor on the SBS threshold powers can be disregarded with fiber core diameter from 20µm to 40µm. In addition, the temperature factor has practically no effect on the corresponding laser output power to SBS threshold power.

Kibria et al [31] found that one of the emerging laser material processing technologies to process cylindrical shaped materials is the laser micro-turning process. This process is used to machine micro-turned groove or surface on the difficult-to-process materials for a specific length of turn along its axis. The present experimental study investigates the laser micro-turning operation of a cylindrical shaped aluminium oxide (Al_2O_3) ceramic to explore the

effect of successive spot overlap and circumferential overlap on the surface roughness (Ra) criterion. Moreover, depth of machining has also been studied by varying various process parameters such as pulse frequency, work piece rotating speed and laser beam average power. Various amounts of spot overlap have been accomplished by different combined settings of related parameters i.e. work piece rotating speed and pulse frequency. In contrast, various circumferential overlap between successive rotational scan widths have been achieved by varying the rotational speed and also axial feed rate of the work piece. Surface roughness (Ra) and machined depth have been measured as output response for machining at various parametric combinations. Analyses have been made through different plots of surface roughness (Ra) and machined depth to study the influence of these overlaps and different process parameters. The experimental results revealed that surface roughness decreases with the increase of both the overlap factors. It is observed from the results that with the increase in circumferential overlap, roughness of the machined surface decreases for each work piece rotating speed setting. Further, wide spot crater is achieved at a higher value of average power. Minimum surface roughness is achieved as 5.25 mm at average power 10 W, pulse frequency 3000 Hz, work piece rotating speed 400 rpm and Y feed rate 0.3 mm/s. The achieved machined depth is high at a low speed of rotation and pulse frequency settings. With the increase of average power of laser beam, the machined depth is found to increase linearly. The maximum micro-turning depth is achieved as 0.146 mm at parametric combination of average power of 10 W, pulse frequency of 3000 Hz, work piece rotating speed of 400 rpm and Y feed rate of 0.3 mm/s.

Satyanarayanan Raghavan et al [32] suggested cost-effective machining of hardened steel components such as a large wind turbine bearing has traditionally posed a significant challenge. This paper presents an approach to machine hardened steel parts efficiently at higher material removal rates and lower tooling cost. The approach involves a twostep process consisting of laser tempering of the hardened workpiece surface followed by conventional machining at higher material removal rates with lower cost ceramic tools to efficiently remove the tempered material. The laser scanning parameters that yield the highest depth oftempered layer are obtained from a kinetic phase change model. Machining experiments are performed to demonstrate the possibility of higher material removal rates and improved tool wear behavior compared to the conventional hard turning process. Tool wear performance, cutting forces, and surface finish of Cubic Boron Nitride (CBN) tools as well as low cost ceramic tools are compared in machining of hardened AISI 52100 steel (~63 HRC). In addition, cutting forces and surface finish are compared for the laser tempering based turning and conventional hard turning processes. Experimental results show the potential benefits of the laser tempering based turning process over the conventional hard turning process.

B. Doloi et al [33] showed an experimental investigation on the effect of process parameters during Nd:YAG laser micro-turning operation of 99% of alumina (Al_2O_3) ceramic materials. Taguchi methodology based experimental design was adopted for carrying out experimentations. The process parameters considered during machining are laser beam average power, pulse frequency, workpiece rotational speed and Y feed rate. Surface

roughness (Ra) and micro-turning depth deviation were considered as the performance criteria for the present experimentation. Analysis of Variance (ANOVA) was performed to find out the significant process parameters during laser micro-turning process. The optimum process parametric settings were obtained by analyzing the signal-to-noise (S/N) ratio values. Experiments on optimal process parametric settings of the responses have been carried out and overall error percentage in S/N ratio calculated is 3.59%. The mathematical model for each of the responses has been developed to predict the mentioned response criteria. Validity of the models have been checked through experiments and the overall error percentages of surface roughness (Ra) and micro-turning depth deviation for validation experiments are 2.83 and 2.96%, respectively. Further experiments have been conducted to study and analyse of the most contributing parameters on respective process criteria.

1.9 OBJECTIVES AND SCOPE OF PRESENT RESEARCH

From the review of past literature it is found that research work has been conducted to find the key influencing parameters of laser machining of different materials like ceramics (aluminium oxide- Al_2O_3, Silicon nitride-Si_3N_4), Metal Matrix Composites (CBN), HSTR alloys like Titanium (Ti), glass reinforced polymers etc. It is also noticed that many experimental works had been carried out for proper understanding of the basic process of laser micro-grooving, surface texturing, micro drilling, laser assisted turning etc. Also turning in different materials and their analysis of the parameters were done but not on Aluminium-1060 alloy as working material. Al-1060 alloy is a very useful material commonly used in the manufacture of chemical equipment and railroad tank cars etc. But this alloy is having very poor machinability if conventional machining is employed. Laser turning process is a potential solution for machining of such alloy. Till date no research work has been reported on laser turning of Al-1060 alloy.

In view of the above objective of the present research study has been framed as follows:

(a) To study the feasibility of the existing pulsed multi-diode pumped fibre laser system for laser turning operation on aluminium-1060 alloy.

(b) To study the basic physics behind the material removal by laser turning.

(c) To design and develop a very high precession (low vibration, minimum eccentricity etc) laser turning set-up which can be integrated with the existing multi diode pump fibre laser machining system.

(d) To explore the influence of various process parameters e.g. feed rate, pulse frequency, average beam power and work piece rotational speed of laser beam turning of aluminium-1060 alloy.

(e) To develop a model in order to predict the response of input factors and to find out the optimal parameter setting for obtaining the best surface finish of the laser turned component.

It is expected that the present research work will open up a new directions of research in the area of laser beam micro-turning of aluminium-1060 alloy and promote advancements in the field of laser beam micro-turning in modern manufacturing industries.

Chapter-2

2. LASER

Laser is acronym for the phenomenon called light amplification by stimulated emission of radiation. The phenomenon was first developed by Albert Einstein. However, the first laser was made possible only in 1960 by Maiman. Since then laser has seen developments.

A laser beam can melt and vaporize diamond when focused by lens system, the energy density being of the order of 100,000 KW/cm^2. Such tremendous energy is released due to certain atoms which have higher energy level and oscillate with particular frequency. The waves absorb energy from the atoms and become highly powerful. Such waves with increased energy are called "Maser" (Microwave Amplification by Stimulated Emission of Radiation). Laser was invented by amplifying ordinary light waves on similar principles i.e. to transmit the light waves with constant frequencies and wavelengths throughout without interference. Such light waves i.e. Laser may be concentrated for the release of tremendous energy.

2.1 LASER OPERATION MECHANISM

Stimulated emission, the underlying concept of laser operation, was first introduced by Einstein in 1917 in one of his three papers on the quantum theory of radiation (Einstein 1917). Almost half a century later, in 1960, T.H. Maiman came up with the first working ruby laser. The three processes required to produce the high-energy laser beam are population inversion, stimulated emission, and amplification.

2.1.1 Population inversion

Population inversion is a necessary condition for stimulated emission. Without population inversion, there will be net absorption of emission instead of stimulated emission. For a material in thermal equilibrium, the distribution of electrons in various energy states is given by the Boltzmann Distribution Law :

$$N_2 = N_1 \exp [- (E_2 - E1) / kT]$$

where N_1 and N_2 are the electron densities in states 1 and 2 with energies E_1 and E_2 respectively. T and k are the absolute temperature and Boltzmann Constant respectively. According to the Boltzmann Law, higher energy states are list populated and population of electrons in higher energy states decreases exponentially with energy. Population inversions corresponding to a non equilibrium distribution of the electrons such that higher energy states have al larger number of electrons than the lower energy states. The process of achieving the population inversion by exciting the electrons to a higher energy states is referred to as Pumping (Svelto and Hanna 1989).
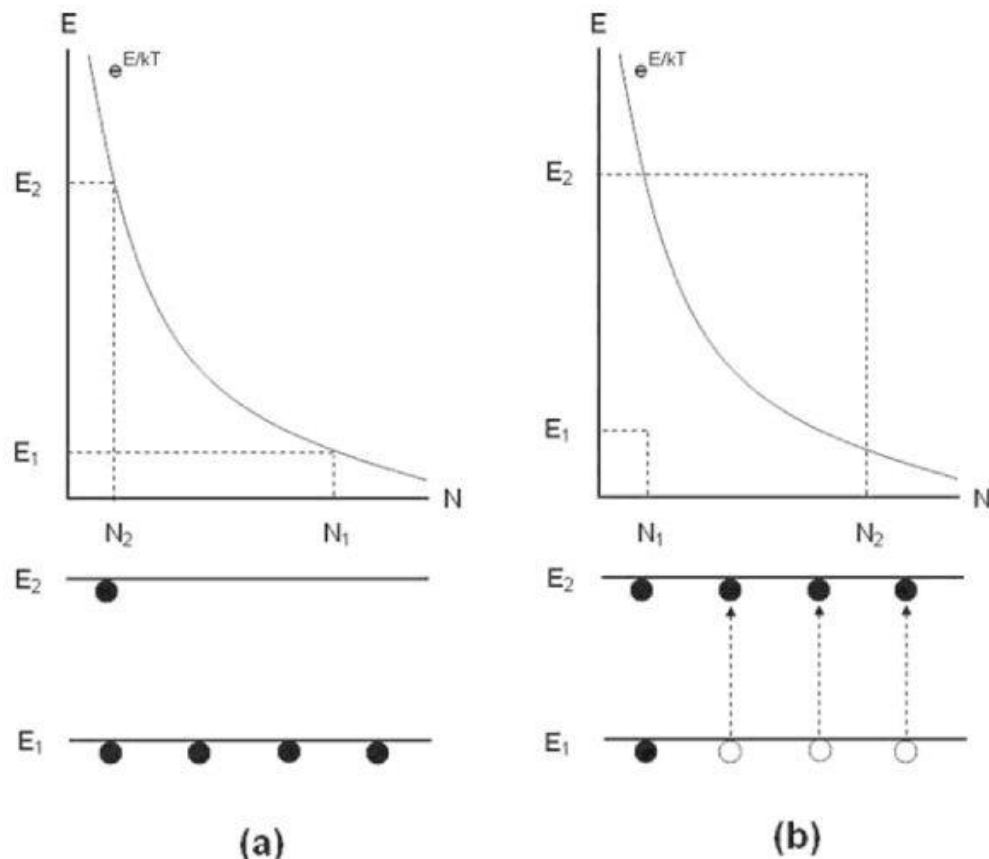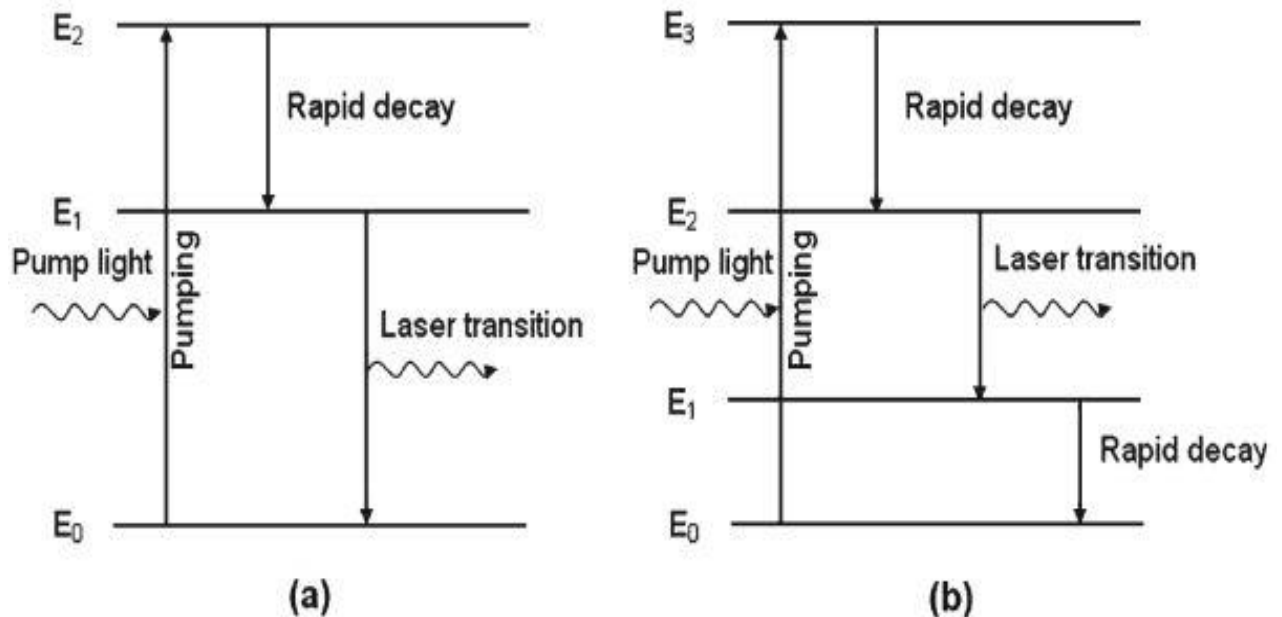

Schematic of the population in two level energy system: (a) thermal equilibrium (b) population inversion

The population inversion explained here is for two level level energy systems. In actual practice it is impossible to achieve population inversion for two level energy systems. Population inversion in most of the lasers involves three or four energy levels.

For a three level energy system, electrons are first pumped from E_0 to E_2 by absorption of radiation from a pumping source. The lifetime of electrons at higher energy level E_2 is very short and electrons from E_2 rapidly decay into a metastable energy level E_1 without any radiation. Thus the net population inversion is achieved between energy levels E_0 and E_1 which is responsible for the subsequent emission of the laser radiation.

Similar mechanism causes population inversion between energy levels E_2 and E_1 in a four level energy systems.

Schematic of the population inversion in (a) three level and (b) four level energy systems

In general population inversion achieved by optical pumping and electrical pumping . In optical pumping gas filled flashlamps are most popular. Flashlamps are essentially quartz or glass tubes filled with gases such as xenon and krypton. Some wavelength of flash matches with absorption characteristics of the active laser medium facilitating population inversion. This is used in solid lasers like ruby and Nd:YAG etc. Typical circuit for flaslamp operation is shown.
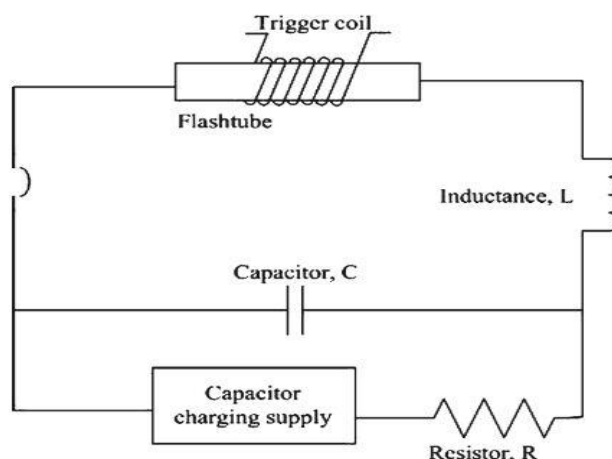

Typical circuitry for flashlamp operation

Recently significant interests have been focused towards using diode lasers of suitable wavelength for pumping the solid state lasers. This led to the development of diode pumped solid state lasers (DPSS). The use of diode lasers offers significant advantages over flashlamps such as better match between the output spectrum of the pumping laser and absorption characteristics of laser medium, increased efficiency, compact and lighter system. Electrical pumping used in gas lasers, is achieved by passing a high voltage electrical current directly through the mixture of active gas medium. The collision of discharge electrons of sufficient high kinetic energy excites one of the gases to high energy level, which subsequently transfer its excitation energy to the second gas through collisions, achieving the population inversion. The minimum population inversion referred to as threshold condition, required for lasing action (Milloni and Eberly 1988).
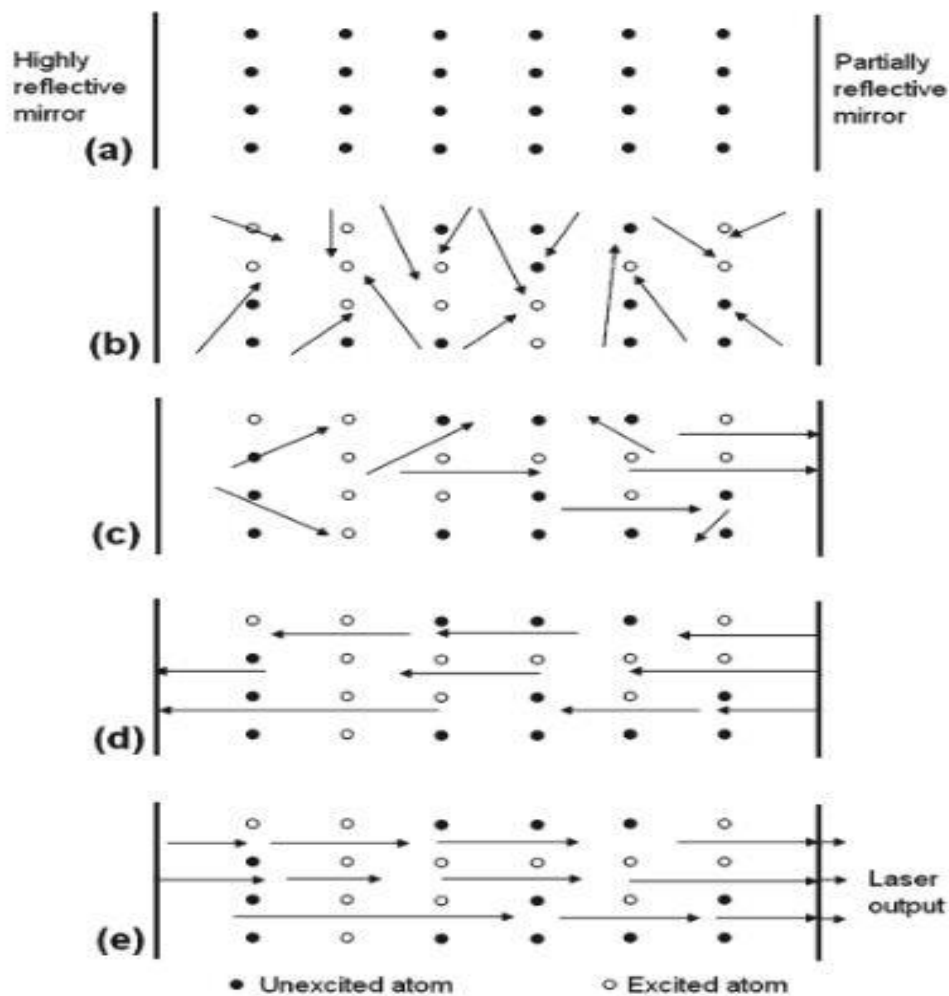
2.1.2 Stimulated emission

Stimulated emission results when incoming photon of frequency υ such that $h\upsilon = (E_2 - E_1)/h$ interacts with the excited atom of active laser medium with population inversion between the states of 1 & 2 with energy E_1 & E_2 respectively. Thus the incoming photon (stimulating photon) triggers the emission of radiation by bringing the atom to a lower energy state. The resulting radiation has the same frequency, direction of travel and phase as that of incoming photon, giving rise to a stream photons (Haken 1983).
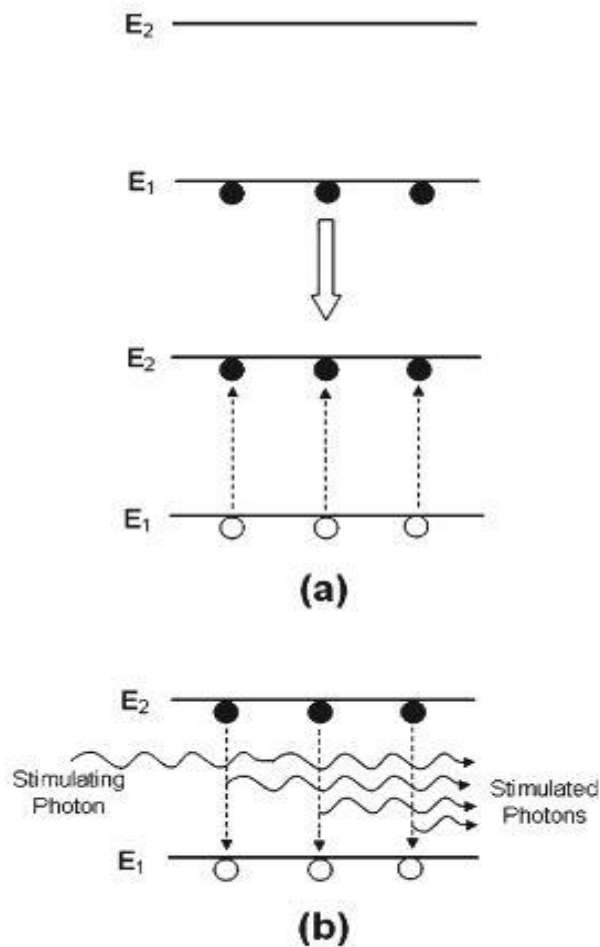
Schematic diagram of laser operation (a) pumping and (b) stimulated emission

31

2.1.3 Amplification

Since the stimulated photons are in the same phase and state of polarization, they add constructively to the incoming photon resulting in an increase in its amplitude. Thus the amplification of the light can be achieved by stimulated by stimulated emission of radiation. Amplification of laser light is accomplished in a resonant cavity consisting of a set of well aligned highly reflecting mirrors at the ends, perpendicular to the cavity axis. The active laser material is placed in between the mirrors. Usually one of the mirrors is fully reflective with reflectivity close to 100% whereas the other mirror has some transmission to allow the laser output to emerge (Thyagarajan and Ghatak 1981). Following figure represents the schematic process of amplification process in the resonator with flat mirrors at the ends and the active laser material in between the mirrors. When the laser is off the optical cavity contains all the laser material in its initial unexcited state. The excitation of atoms (Population Inversion) is soon achieved by optical pumping followed by initiation of stimulated emission. The intensity of stimulated radiation is increased as it travels to the end of the mirrors. Further amplification is achieved by reflecting the photons into the active medium. The photons travel long path back and forth through the lasing medium stimulating more and more emissions resulting in high intensity laser beam output from one of the mirror (Chryssolouris 1991).

Schematic of amplification stages during operation : (a) initial un excited state (laser off), (b) optical pumping resulting in excited state, (c) initiation of stimulated emission, (d) continued amplification due to repeated reflection from the end mirrors resulting in subsequent laser output from one end of the mirror.

2.2   PROPERTIES OF LASER RADIATION

The laser is characterized by a number of interesting properties. Various applications of lasers exploit specific combinations of the laser properties. This section briefly explains the most important property of laser light.

2.2.1 Monochromaticity

Monochromaticity is the most important property of laser beam and is measured in terms of spectrum line widths. The laser output consists of very closed spaced, discrete and narrow spectral lines which satisfies the resonance condition given by $d = n\lambda/2$ where d is the cavity length, n is an integer and λ is the wavelength. Monochromaticity is due to narrow spectral widths of individual modes. A laser can be constructed to operate in only one longitudinal mode to give better monocromaticity (Ready 1997).

2.2.2 Collimation

Collimation of the laser is related with the directional nature of the beam. Highly directional beams are called highly collimated beams which can be focused on a very small area even at longer distances. Hence energy can be efficiently collected on a small area without much loss of beam intensity. The degree of collimation is directly related with the beam divergence angles (Duley 1983). Ideally the divergence angle should be zero for highest collimation. However this is impossible due to physical limits set by diffraction phenomenon. The beam divergence angles for most of the lasers (except semiconductor lasers) range from 0.2 to 10 milliradians.

2.2.3 Beam coherence

Coherence is the degree of orderliness of waves and specified in terms of mutual coherence function which is a measure of the correlation between the light wave at two points at two different times. Coherence can be of two types: spatial and temporal coherence. Spatial coherence correlates the phases at different points in a space at a single moment in time, whereas temporal coherence correlates the phases at a single point in space over a period of time. Coherence properties can be improved by operating the laser in a single longitudinal and transverse mode.

2.2.4 Brightness or radiance

Brightness or radiance is defined as the amount of power emitted per unit area per unit solid angle. Laser beams are emitted into very small divergence angles in the range of 10^{-6} steradians, hence it can be focused on a very small area ensuring the correspondingly high brightness of laser beams. Brightness of the laser beam is a very important factor in material processing and determines the intensity or energy density of the laser beam. The brightness of the source cannot be increased by the optical system, however high brightness characteristics are influenced by operating the lasers in Gaussian mode with minimum divergence angle and high output power.

2.2.5 Focal spot size

The spot radius is the distance from the axis of the beam to the point at which the intensity drops to a lower value at the centre of the beam. Focal spot size determines the irradiance, which is the prime importance in material processing. For example the dominant mechanism of material removal during laser machining such as surface melting or evaporation and consequent rate of material removal directly depends on the irradiance at the surface. The maximum irradiance corresponds to minimum diameter of spot. However it is not possible to focus the beam to an infinitesimal point and there is always a minimum spot size determined by diffraction limit.

2.2.6 Transverse modes

The cross section of laser beams exhibit certain distinct spatial profiles termed as transverse modes and are represented as Transverse Electromagnetic Mode TEM_{mn} where m and n are small integers representing the no of nodes in direction orthogonal to direction of propagation of beam. The various transverse modes are shown in following figure. The fundamental mode TEM_{00} has Gaussian Spatial Distribution and is most commonly used mode in machining applications. The intensity distribution of the Gaussian beam can be expressed as:

$I(r) = I_0 \exp [-2r^2 / w^2]$ where r is radius of the beam, I_0 is the intensity of the beam at r = 0, and w is the radius of the beam at which $I = I_0 e^{-2}$.
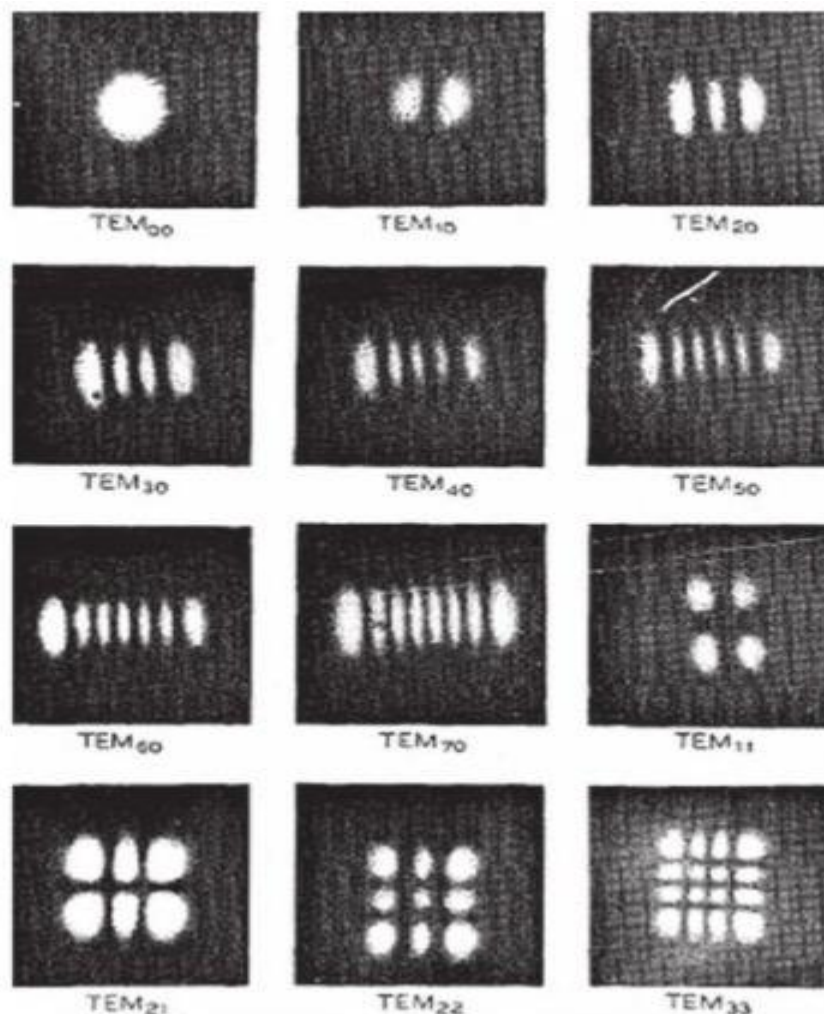
Spatial Modes of Laser Operation

2.3   LASING MATERIAL

Many materials exhibit lasing action. However a limited number is used in metal working. Solids, liquids and gases can be used as lasing materials. The lasers are also classified according to the type of material used. In metal working solid state and gas lasers are generally used.

Solid state lasers consist of a host material which may be crystalline solid or glass doped with an active material whose atom provides the lasing action. For example the Nd-YAG laser consists of a single neodymium. In ruby laser the aluminium oxide contains Cr^{3+} ions as active material.

Solid state lasers pumped optically, generally by flash tube. The flash tubes are mounted in a reflecting cavity parallel to the lasing rod.

In one of the arrangement, two flash or even more flash tubes are maintained on the foci of an elliptical reflecting cavity with the lasing rod parallel to central axis. Gas lasers consist of optically transparent tube fitted with a single gas or a mixture of gases of the lasing material. The gases used commercially are He-Ne, Argon, CO_2 etc. The power source is the electric discharge between electrodes or flash tubes.

The power output is dependent on the length of the laser tube. Thus CO_2 laser can develop about 50 W for every meter length of the tube. The problem of length could be overcome by arranging the short length tubes in a zig zag fashion with a reflecting surface at each end. Thus Ferranti Electric Inc. developed 400 W CO_2 laser in a length of 120 m. A typical high power CO_2 laser contains three gases, namely CO_2, N_2 and He. CO_2 gives the molecular action to generate photons, N_2 reinforces and sustains this action and He provides intra cavity cooling. In gas lasers stabilization of discharge is very necessary which requires cooling of gas. There are also other types of gas laser with axial gas flow and cross gas flow arrangements.

Lasers are now available in a variety of power ratings i.e. from a few mill watts to 20 kW in the continuous wave (CW) mode and in much higher intensity in pulsed mode. Laser action can be obtained over the entire frequency range from ultraviolet to infrared. Lasers commonly used in metal working have wavelengths ranging from 0.6 µm to 10.6 µm.

2.4 TYPES OF LASERS AND THEIR WORKING PRINCIPLES

(a)   Excimer lasers

Excimer lasers are a special sort of gas laser powered by an electric discharge in which the lasing medium is an excimer, or more precisely an exciplex in existing designs. These are molecules which can only exist with one atom in an excited electronic state. Once the molecule transfers its excitation energy to a photon, therefore, its atoms are no longer bound to each other and the molecule disintegrates. This drastically reduces the population of the lower energy state thus greatly facilitating a population inversion. Excimers currently used are all noble gas compounds; noble gasses are chemically inert and can only form compounds while in an excited state. Excimer lasers typically operate at ultraviolet wavelengths with major applications including semiconductor photolithography and LASIK eye surgery. Commonly used excimer molecules include ArF (emission at 193 nm), KrCl (222 nm), KrF (248 nm), XeCl (308 nm), and XeF (351 nm).

(b)   Solid state lasers

Solid-state lasers use a crystalline or glass rod which is "doped" with ions that provide the required energy states. For example, the first working laser was a rubylaser, made from ruby (chromium-doped corundum). The population inversion is actually maintained in the "dopant", such as chromium or neodymium. These materials are pumped optically using a shorter wavelength than the lasing wavelength, often from a flashtube or from another laser. It should be noted that "solid-state" in this sense refers to a crystal or glass, but this usage is distinct from the designation of "solid-state electronics" in referring to semiconductors. Semiconductor lasers (laser diodes) are pumped electrically and are thus not referred to as solid-state lasers. The class of solid-state lasers would, however, properly include fiber lasers in which dopants in the glass lase under optical pumping. But in practice these are simply referred to as "fiber lasers" with "solid-state" reserved for lasers using a solid rod of such a material. Neodymium is a common "dopant" in various solid-state laser crystals, including yttrium orthovanadate (Nd:YVO4), yttrium lithium fluoride (Nd:YLF) and yttrium aluminium garnet (Nd:YAG). All these lasers can produce high powers in the infrared spectrum at 1064 nm. They are used for cutting, welding and marking of metals and other materials, and also in spectroscopy and for pumping dye lasers. These lasers are also commonly frequency doubled, tripled or quadrupled, in so called "diode pumped solid state" or DPSS lasers. Under second, third, or fourth harmonic generation these produce 532 nm (green, visible), 355 nm and 266 nm (UV) beams.
This is the technology behind the bright laser pointers particularly at green (532 nm) and other short visible wavelengths. Titanium-doped sapphire (Ti:sapphire) produces a highly tunable infrared laser, commonly used for spectroscopy. It is also notable for use as a mode-locked laser producing ultra short pulses of extremely high peak power. Thermal limitations in solid state lasers arise from unconverted pump power that manifests itself as heat. This heat, when coupled with a high thermo-optic coefficient (dn/dT) can give rise to thermal lensing as well as reduced quantum efficiency. These types of issues can be overcome by another novel diode-pumped solid-state laser, the diode-pumped thin disk laser. The thermal limitations in this laser type are mitigated by using a laser medium geometry in which the thickness is much smaller than the diameter of the pump beam. This allows for a more even thermal gradient in the material. Thin disk lasers have been shown to produce up to kilowatt levels of power.

(c) Gas lasers

Gas lasers are one of the oldest types of laser. Gas lasers using many different gases have been built and used for many purposes. The helium-neon laser (HeNe) is able to operate at a number of different wavelengths, however the vast majority are engineered to lase at 633 nm; these relatively low cost but highly coherent lasers are extremely common in optical research and educational laboratories. Carbon dioxide (CO_2) lasers can emit many hundreds of watts in a single spatial mode which can be concentrated into a tiny spot. This emission is in the thermal infrared at 10.6 μm; such lasers are regularly used in industry for cutting and welding. The efficiency of a CO2 laser is unusually high: over 30%. Argon-ion lasers can operate at a number of lasing transitions between 351 and 528.7 nm. Depending on the optical design one or more of these transitions can be lasing simultaneously; the most commonly used lines are 458 nm, 488 nm and 514.5 nm. Helium-neon laser was the first laser to be operated and is the most important gas laser even today. Fig shows the internal design of hard sealed helium neon laser.
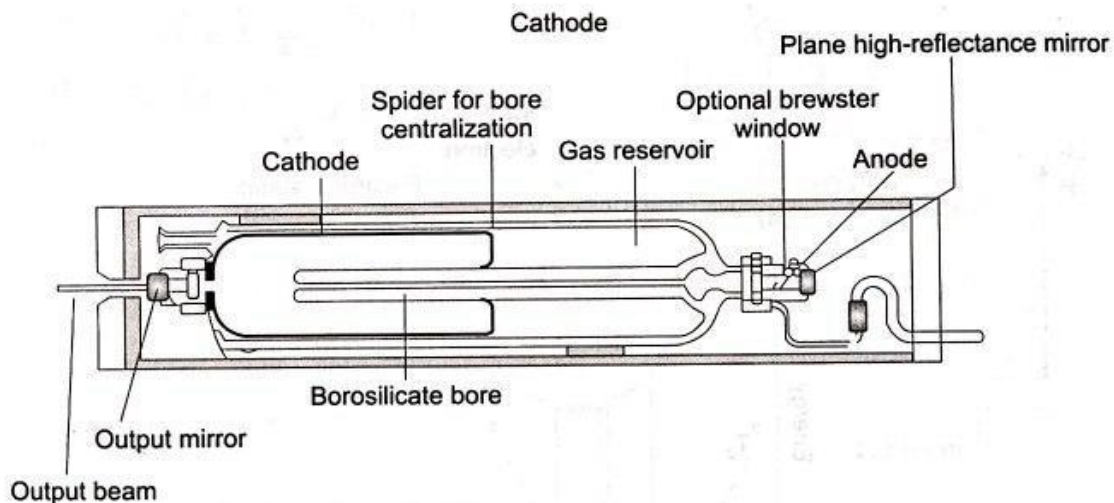

Fig: Internal design of hard sealed helium neon laser

A nitrogen transverse electrical discharge in gas at atmospheric pressure (TEA) laser is an inexpensive gas laser, often home-built by hobbyists, which produces rather incoherent UV light at 337.1 nm. Metal ion lasers are gas lasers that generate deep ultraviolet wavelengths. Helium silver (HeAg) 224 nm and neoncopper (NeCu) 248 nm are two examples. These lasers have quite narrow oscillation line widths, less than 3 GHz (0.5 picometers), making them candidates for use in fluorescence suppressed Raman spectroscopy.

(d)   Chemical lasers

In the search of alternative methods to the convention excitation of materials with light sources, scientists have found that the Intense light produced by reactive chemicals can be used for laser excitation. A chemical laser produces a high energy beam from the energy released in the reaction of two or more chemicals. It converts the free energy produced by a chemical reaction into a specific excitation of some product species Such chemical reactions can be brought about with the aid of gamma rays, electrons, photons etc. Flames can also be

used as a source of excitation to initiate teaser action. Explosive gas mixture, which may also be used to excite laser radiation in the gas itself, is another pumping source. Chemical laser is potentially a very efficient compact device. In a typical chemical laser, nitrogen is heated by an electric arc and mixed with sulphur hexafluoride. The heated mixture is then forced through a set of nozzles and hydrogen is injected into the exhaust. Lasing takes place when the exhaust passes between two mirrors. The laser emission was obtained in the infrared region with the help of the energy produced by the reaction of hydrogen and chlorine. The hydrogen fluoride laser is another very powerful chemical laser which produces laser radiation at wavelengths from 2.6-3.5 μm. A mixture of hydrogen and fluorine is used in this laser. When the fluorine molecule is dissociated optically or by discharge or by electron beam pumping, a chain of chemical reactions takes place reducing the vibrationally-excited hydrogen fluoride molecule. Since there are no hydrogen fluoride molecules in the lower state in the beginning, the population inversion is easily achieved and the laser action takes place. The deuterium fluoride laser is another important chemical laser. Its working is similar to that of the hydrogen fluoride laser. It produces laser radiation in the region 3.5-4.1 μm. The chemical laser produces such a large amount of energy in relation to its size that it very much in the running as a potential laser weapon. Weight by weight, chemical energy sources yields about 1,000,000 joules per pound as against the conventional electrical pumping sources which yield about 100 joules per pound. Because of their high efficiency and very powerful beams, chemical lasers are being developed for star war programme by the US to destroy the enemy missiles during their journey in space.

(e) Fibre lasers

Solid-state lasers or laser amplifiers where the light is guided due to the total internal reflection in a single mode optical fibre are instead called fibre lasers. Guiding of light allows extremely long gain regions providing good cooling conditions; fibbers have high surface area to volume ratio which allows efficient cooling. In addition, the fibre wave guiding properties tend to reduce thermal distortion of the beam. Erbium and ytterbium ions are common active species in such lasers. Quite often, the fibre laser is designed as a double-clad fibre. This type of fibre consists of a fibre core, an inner cladding and an outer cladding. The index of the three concentric layers is chosen so that the fibre core acts as a single-mode fibre for the laser emission while the outer cladding acts as a highly multimode core for the pump laser. This lets the pump propagate a large amount of power into and through the active inner core region, while still having a high numerical aperture (NA) to have easy launching conditions. Pump light can be used more efficiently by creating a fibre disk laser, or a stack of such lasers. Fibre lasers have a fundamental limit in that the intensity of the light in the fibre cannot be so high that optical nonlinearities induced by the local electric field strength can become dominant and prevent laser operation and/or lead to the material destruction of the fibre. This effect is called photo darkening. In bulk laser materials, the cooling is not so efficient, and it is difficult to separate the effects of photo darkening from the thermal effects, but the experiments in fibbers show that the photo darkening can be attributed to the formation of long living colour centres.

(f) Dye lasers

The dye lasers are made up of organic substances which absorb in the optical region. The active medium is a solution of organic dye which is made by solvents like water, ethanol, methanol, benzene, acetone etc. Rhodium 6G is the common dye used in a dye laser. A dye

laser consists of an organic dye mixed with a solvent, which may be circulated through a dye cell, or streamed through open air using a dye jet. A high energy source of light is needed to 'pump' the liquid beyond its lasing threshold. A fast discharge flash lamp or an external laser is usually used for this purpose. Mirrors are also needed to oscillate the light produced by the dye's fluorescence, which is amplified with each pass through the liquid. The output mirror is normally around 80% reflective, while all other mirrors are usually more than 99.9% reflective. The dye solution is usually circulated at high speeds, to help avoid triplet absorption and to decrease degradation of the dye. A prism or diffraction grating is usually mounted in the beam path, to allow tuning of the beam. Because the liquid medium of a dye laser can fit any shape, there are a multitude of different configurations that can be used.

(g)   Semiconductor lasers

Semiconductor lasers are diodes which are electrically pumped. Recombination of electrons and holes created by the applied current introduces optical gain. Reflection from the ends of the crystal forms an optical resonator, although the resonator can be external to the semiconductor in some designs. Commercial laser diodes emit at wavelengths from 375 nm to 3500 nm. Low to medium power laser diodes are used in laser pointers, laser printers and CD/DVD players. Laser diodes are also frequently used to optically pump other lasers with high efficiency. The highest power industrial laser diodes, with power up to 10 kW (70dBm), are used in industry for cutting and welding. External-cavity semiconductor lasers have a semiconductor active medium in a larger cavity. These devices can generate high power outputs with good beam quality, wavelength-tunable narrow-line width radiation, or ultra short laser pulses. Vertical cavity surface-emitting lasers (VCSELs) are semiconductor lasers whose emission direction is perpendicular to the surface of the wafer. VCSEL devices typically have a more circular output beam than conventional laser diodes, and potentially could be much cheaper to manufacture. As of 2005, only 850 nm VCSELs are widely available, with 1300 nm VCSELs beginning to be commercialized, and 1550 nm devices an area of research. VECSELs are external cavity VCSELs. Quantum cascade lasers are semiconductor lasers that have an active transition between energy sub-bands of an electron in a structure containing several wells. The development of a silicon laser is important in the field of optical computing. Silicon is the material of choice for integrated circuits, and so electronic and silicon photonic components (such as optical interconnects) could be fabricated on the same chip. Unfortunately, silicon is a difficult lasing material to deal with, since it has certain properties which block lasing. However, recently teams have produced silicon lasers through methods such as fabricating the lasing material from silicon and other semiconductor materials, such as indium(III) phosphide or gallium(III) arsenide, materials which allow coherent light to be produced from silicon. These are called hybrid silicon laser. Another type is a Raman laser, which takes advantage of Raman scattering to produce a laser from materials such as silicon.

(h)   Free electron lasers

Free-electron lasers, discovered recently, are significantly different from any other type of laser in that the laser radiation is not obtained by discreet transitions in atoms or molecules of a material. Instead, a high-energy beam of electrons (of the order of one million electron volts (meV)) is directed to pass through a spatially varying magnetic field that causes the electrons to oscillate back and forth in a direction transverse to the direction of their beam, at a frequency related to the energy of the electron beam. This oscillation causes the electrons to

radiate at the oscillation frequency and to stimulate other electrons also to oscillate and radiate at the same frequency, in phase with the original oscillating electrons thereby producing an intense beam of light emerging from one end of the device. Mirrors can be placed at the ends of the magnetic region to feed the optical beam back through the amplifier to stimulate more radiation and cause the beam to grow. A great advantage of the free electron laser is that a high average output power of the range of a few kilowatts can be obtained in the continuous mode.

2.5 MODES OF OPERATION

Depending upon the power output a laser can be classified as operating in either continuous or pulsed mode. Of course even a laser whose output is normally continuous can be intentionally turned on and off at some rate in order to create pulses of light. When the modulation rate is on time scales much slower than the cavity lifetime and the time period over which energy can be stored in the lasing medium or pumping mechanism, then it is still classified as a "modulated" or "pulsed" continuous wave laser. Most laser diodes used in communication systems fall in this category. There are three modes of operation:

    (a) Continuous wave operation (CW)
   (b) Pulsed operation
    (c) Pulsed pumping

Chapter-3

3. FIBRE LASER SYSTEM

A fibre laser or fibre laser is a laser in which the active gain medium is an optical fibre doped with rareearthelements suchas erbium, ytterbium, neodymium,dysprosium, praseodymium, thulium and holmium. They are related to doped fibre amplifiers, which provide light amplification without lasing. Fibre nonlinearities, such as stimulated Raman scattering or four-wave mixing can also provide gain and thus serve as gain media for a fibre laser.

3.1 HISTORY OF FIBRE LASER

Fibre laser is a laser in which the active gain medium is an optical fibre doped with rare earth elements such as erbium, ytterbium, neodymium, dysprosium, praseodymium, and thulium. They are related to doped fibre amplifiers, which provide light amplification without lasing. Fibre nonlinearities, such as stimulated Raman scattering or four wave mixing can also provide gain and thus serve as gain media for a fibre laser. Improvement of fibre laser can be shown as below:
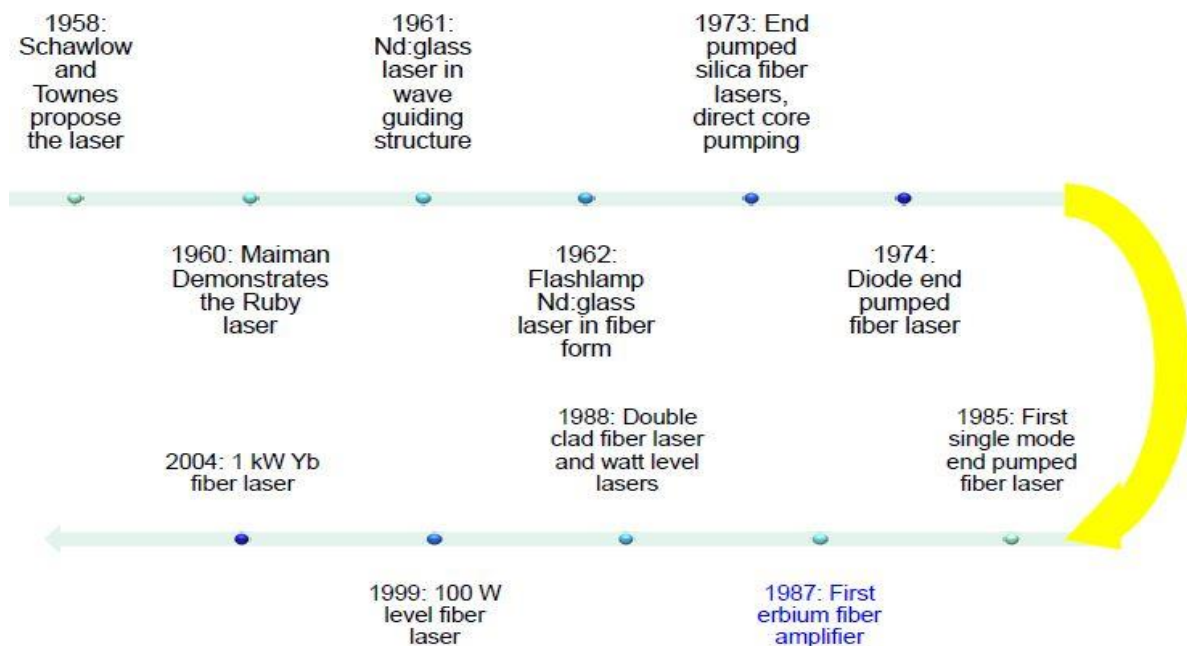
3.2 TYPES OF FIBRE LASER
- DC Fibres
- SM Fibres
- Assembled Fibres
- PM Fibres
- MM Fibre

3.3 DESIGN AND MANUFACTURE OF FIBRE LASER

Unlike most other types of lasers, the laser cavity in fibre lasers is constructed monolithically by fusion splicing different types of fibre; fibre Bragg gratings replace conventional dielectric mirrors to provide optical feedback. Another type is the single longitudinal mode operation of ultra narrow distributed feedback lasers (DFB) where a phase-shifted Bragg grating overlaps the gain medium. Fibre lasers are pumped by semiconductor laser diodes or by other fibre lasers. Q-switched pulsed fibre lasers offer a compact, electrically efficient alternative to Nd:YAG technology.

Double clad- fibres:

Many high-power fibre lasers are based on double-clad fibre. The gain medium forms the core of the fibre, which is surrounded by two layers of cladding. The lasing mode propagates in the core, while a multimode pump beam propagates in the inner cladding layer. The outer cladding keeps this pump light confined. This arrangement allows the core to be pumped with a much higher-power beam than could otherwise be made to propagate in it, and allows the conversion of pump light with relatively low brightness into a much higher-brightness signal. As a result, fibre lasers and amplifiers are occasionally referred to as "brightness converters." There is an important question about the shape of the double-clad fibre; a fibre with circular symmetry seems to be the worst possible design. The design should allow the core to be small enough to support only few (or even one) modes. It should provide sufficient cladding to confine the core and optical pump section over a relatively short piece of the fibre.

Power scaling:

Recent developments in fibre laser technology have led to a rapid and large rise in achieved diffraction-limited beam powers from diode-pumped solid-state lasers. Due to the introduction of large mode area (LMA) fibres as well as continuing advances in high power and high brightness diodes, continuous-wave single-transverse-mode powers from Yb-doped fibre lasers have increased from 100 W in 2001 to >20 kW. Commercial single-mode lasers have reached 10 kW in CW power. In 2014 a combined beam fibre laser demonstrated power of 30 kW.

Mode locking:

1. Passive mode locking:

[i] Nonlinear polarization rotation : When linearly polarized light is incident to a piece of weakly birefringent fibre, the polarization of the light will generally become elliptically polarized in the fibre. The orientation and ellipticity of the final light polarization is fully determined by the fibre length and its birefringence. However, if the intensity of the light is strong, the non-linear optical Kerr effect in the fibre must be considered, which introduces extra changes to the light polarization. As the polarization change introduced by the optical Kerr effect depends on the light intensity, if a polarizer is put behind the fibre, the light intensity transmission through the polarizer will become light intensity dependent. Through appropriately selecting the orientation of the polarizer or the length of the fibre, an artificial

saturable absorber effect with ultra-fast response could then be achieved in such a system, where light of higher intensity experiences less absorption loss on the polarizer. The NPR technique makes use of this artificial saturable absorption to achieve the passive mode locking in a fibre laser. Once a mode-locked pulse is formed, the non-linearity of the fibre further shapes the pulse into an optical soliton and consequently the ultrashort soliton operation is obtained in the laser. Soliton operation is almost a generic feature of the fibre lasers mode-locked by this technique and has been intensively investigated.

[ii] Semiconductor saturable absorber mirrors (SESAMs) : Semiconductor saturable absorbers were used for laser mode-locking as early as 1974 when p-type germanium is used to mode lock a $CO2$ laser which generated pulses ~500 ps . Modern SESAMs are III-V semiconductor single quantum well (SQW) or multiple quantum wells grown on semiconductor distributed Bragg reflectors (DBRs). They were initially used in a Resonant Pulse Mode locking (RPM) scheme as starting mechanisms for Ti:Sapphire lasers which employed KLM as a fast saturable absorber . RPM is another coupled-cavity mode-locking technique. Different from APM lasers which employ non-resonant Kerr-type phase nonlinearity for pulse shortening, RPM employs the amplitude nonlinearity provided by the resonant band filling effects of semiconductors. SESAMs were soon developed into intracavity saturable absorber devices because of more inherent simplicity with this structure. Since then, the use of SESAMs has enabled the pulse durations, average powers, pulse energies and repetition rates of ultrafast solid-state lasers to be improved by several orders of magnitude. Average power of 60 W and repetition rate up to 160 GHz were obtained. By using SESAM-assisted KLM, sub-6 fs pulses directly from a Ti: Sapphire oscillator was achieved. A major advantage SESAMs have over other saturable absorber techniques is that absorber parameters can be easily controlled over a wide range of values. For example, saturation fluence can be controlled by varying the reflectivity of the top reflector while modulation depth and recovery time can be tailored by changing the low temperature growing conditions for the absorber layers . This freedom of design has further extended the application of SESAMs into modelocking of fiber lasers where a relatively high modulation depth is needed to ensure self-starting and operation stability. Fibre lasers working at 1 µm and 1.5 µm were successfully demonstrated.

[iii] Carbon nanotube saturable absorbers

[iv] Graphene saturable absorbers

Active Mode Locking:

Active mode-locking is normally achieved by modulating the loss (or gain) of the laser cavity at a repetition rate equivalent to the cavity frequency, or a harmonic thereof. In practice, the modulator can be acousto-optic or electro-optic modulator, Mach-Zehnder integrated-optic modulators, or a semiconductor electro-absorption modulator (EAM). The principle of active mode-locking with a sinusoidal modulation. In this situation, optical pulses will form in such a way as to minimize the loss from the modulator. The peak of the pulse would automatically adjust in phase to be at the point of minimum loss from the modulator. Because of the slow variation of sinusoidal modulation, it is not very straightforward for generating ultrashort optical pulses (< 1ps) using this method.

Dark soliton fibre lasers:

In the non-mode locking regime, the first dark soliton fibre laser has been successfully achieved in an all-normal dispersion erbium-doped fiber laser with a polarizer in cavity. Experimentally finding that apart from the bright pulse emission, under appropriate conditions the fiber laser could also emit single or multiple dark pulses. Based on numerical simulations we interpret the dark pulse formation in the laser as a result of dark soliton shaping.

Multiwavelength fiber lasers:

Recently,multiwavelength dissipative soliton in an all normal dispersion fiber laser passively mode-locked with a SESAM has been generated. It is found that depending on the cavity birefringence, stable single-, dual- and triple-wavelength dissipative soliton can be formed in the laser. Its generation mechanism can be traced back to the nature of dissipative soliton.

Fiber disk lasers:

Another type of fibre laser is the fibre. In such lasers, the pump is not confined within the cladding of the fibre, but instead pump light is delivered across the core multiple times because the core is coiled on itself like a rope. This configuration is suitable for power scaling in which many pump sources are used around the periphery of the coil. Fibre disk lasers have exceptional protection against back reflection compared to traditional fibre lasers. Fibre disk lasers can be used for welding and cutting applications requiring more than 1000 watts of power.

3.4 OUTLINE OF AN ERBIUM DOPED FIBRE AMPLIFIER
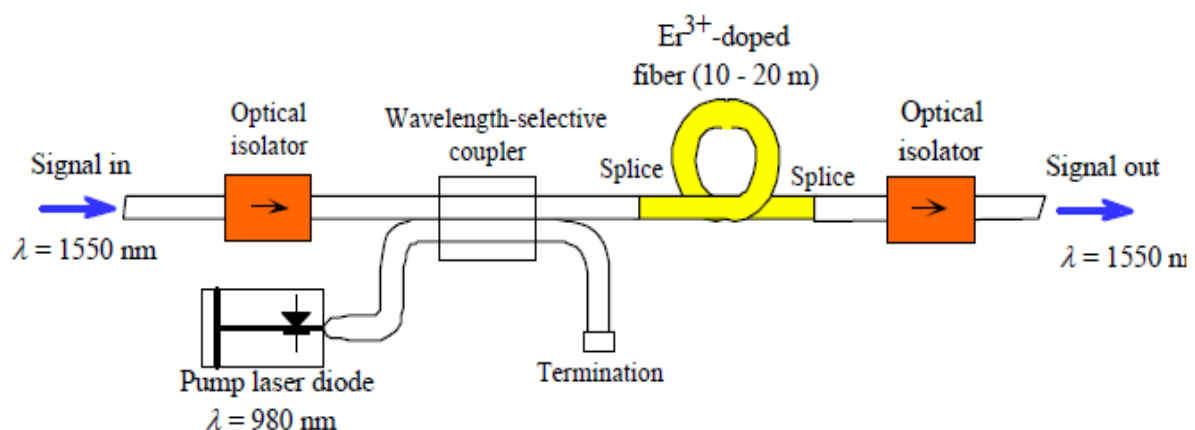
3.5 ADVANTAGES OF FIBRE LASER

The advantages of fibre lasers over other types include:

- Light is already coupled into a flexible fibre: The fact that the light is already in a fibre allows it to be easily delivered to a movable focusing element. This is important for laser cutting, welding, and folding of metals and polymers.
- High output power: Fibre lasers can have active regions several kilometres long, and so can provide very high optical gain. They can support kilowatt levels of continuous output power because of the fibre's high surface area to volume ratio, which allows efficient cooling.
- High optical quality: The fibre's wave guiding properties reduce or eliminate thermal distortion of the optical path, typically producing a diffraction-limited, high-quality optical beam.
- Compact size: Fibre lasers are compact compared to rod or gas lasers of comparable power, because the fibre can be bent and coiled to save space.
- Reliability: Fibre lasers exhibit high vibrational stability, extended lifetime, and maintenance-free turnkey operation.
- High peak power and nanosecond pulses enable effective marking and engraving.
- The additional power and better beam quality provide cleaner cut edges and faster cutting speeds.
- Lower cost of ownership.
- Fiber lasers are now being used to make high-performance surface-acoustic wave (SAW) devices. These lasers raise throughput and lower cost of ownership in comparison to older solid-state laser technology.

Doped core as an amplifier medium

Fiber Bragg gratings
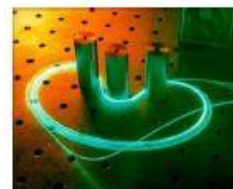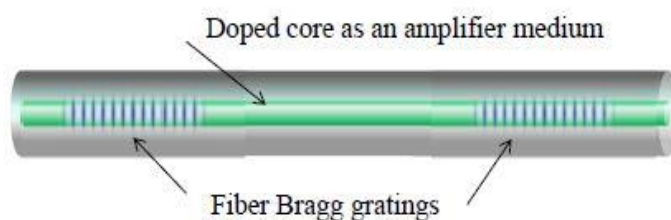
Simplicity – Flexibility – Versatility – Performance

- No free space cavity alignment
- Exceptional reliability
- Low maintenance

- Standard wall plug operation
- With high wall plug efficiency (~30%)
- High beam quality
- Direct fiber delivery

IPG

SPI (TRUMPF)

3.6 APPLICATIONS OF FIBRE LASER

Fibre laser can also refer to the machine tool that includes the fibre resonator. Applications of fibre lasers include the following fields:

    (i)   Material processing (marking, engraving, cutting),
    (ii)   Telecommunications,
    (iii)   Spectroscopy,
    (iv)   Medicine,
    (v)   Directed energy weapons.

3.7 FIBRE LASER MACHINING SET UP

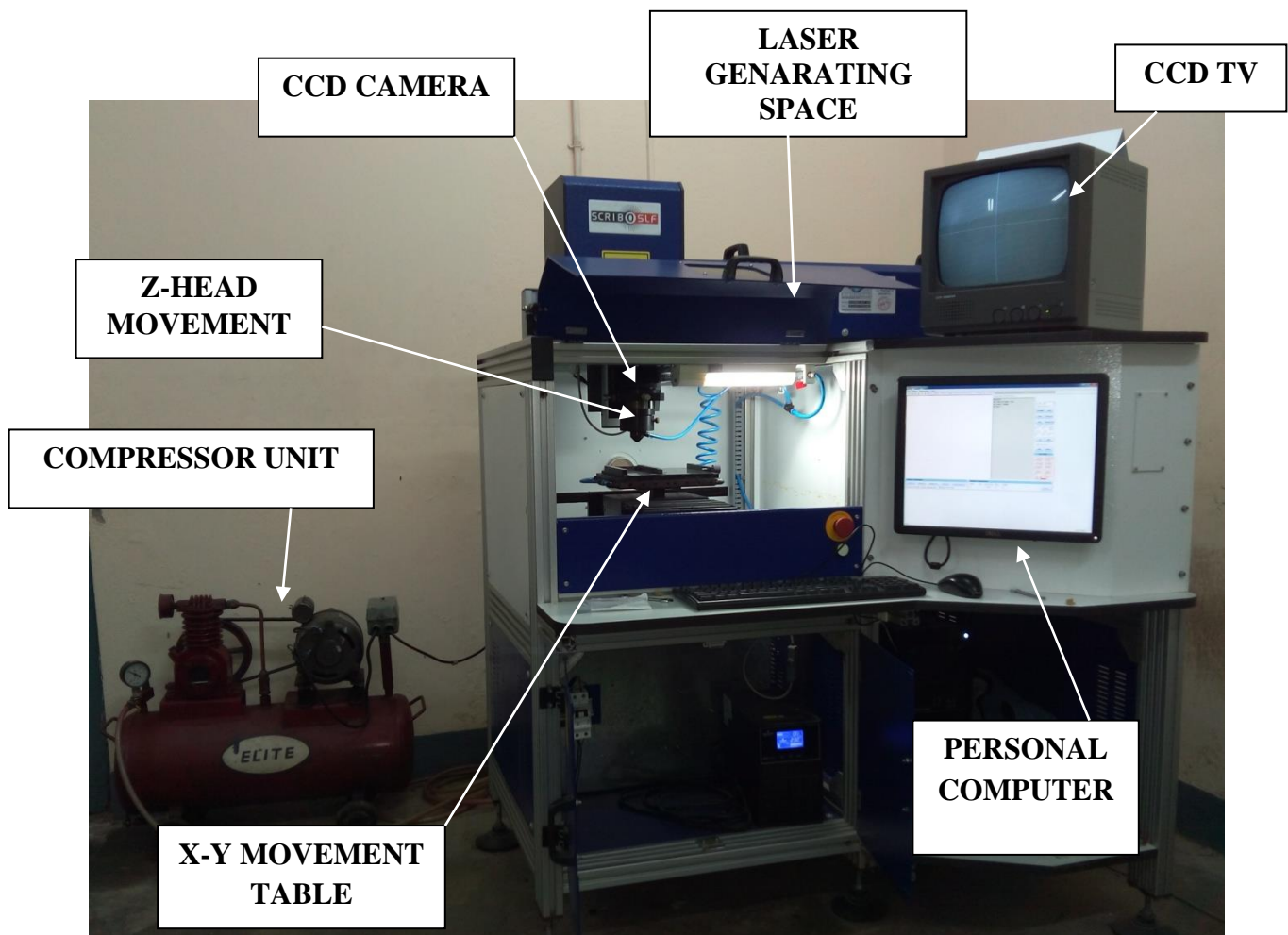## Shajanand Multi Diode Pumped Fibre Laser

Figure: Photographic View of the Laser Machining Set up

47

Technical Specification

Laser	Multi Diode Pump Fibre Laser
Nominal Average Power	20 W
Max Peak Power	7.5 KW
Pulse Repetition Rate	20-80 KHz
Wavelength	1064 nm
Pulse duration @20 KHz	<120 ns
Power Stability	>95 %
Pulse Energy @ 20KHz	1mj
Inbuilt Guide Laser	0.5mW, =660nm
Beam Quality	1.5 (M2)

Components of erbium doped fibre laser:

Power supply with Isolation Transformer

Isolation transformer converts the main power supply from AC to DC

Fig: Photographic view of isolation transformer

Laser source

Fibre laser is pumped with special high power multimode diodes via cladding surrounding as single mode core. Life of this individual multimode diode is quite long corresponding to conventional diode pump solid-state laser (DPSSL). Fibre laser is pumped by multiple identical diodes all feeding same gain medium, whereas DPSSL is pumped by a single diode bar. In the unlikely event of failure of any single pump diode in the fibre laser, the laser continues to work with slightly lower specification. In case of DPSSL, the total laser fails if diode stops working.

Beam delivery system

The biggest benefit of fibre laser is that the Gain Medium is fibre & delivery is also through the fibre. This leads to less chances of failure at coupling point between gain medium and delivery when extended to the workplace.

Rotational speed control unit

For carry out experiment at different parametric setting a rpm controller unit is attached separately to vary the speed between a range. Here we can change the rpm by changing the knob below the display unit.

Fig: Photographic view of work piece rpm control unit

Laser beam focussing control system

By changing the focal length of the focusing lens one can alter the power density and the depth of focus produced by the laser of given beam diameter. A lower focal length lens has higher power density but large depth of focus for as same beam diameter falling over a focusing lens. The alignment of the focusing lens is very important because if the beam centre is not coincident with the centre of the lens then the beam after the lens will not be straight and therefore the cutting efficiently drastically decreases. To get proper focus on the work piece this Fibre laser system equipped with CNC interface, CCD camera, CCTV.

CNC controller for axis movement

An X-Y table and the movement of X and Y-axis is controlled by CNC controller unit, for proper focusing of laser beam by means of focusing lens. The hardware specification of CNC table unit is shown in table2. Z axis controls the focus length of the job.
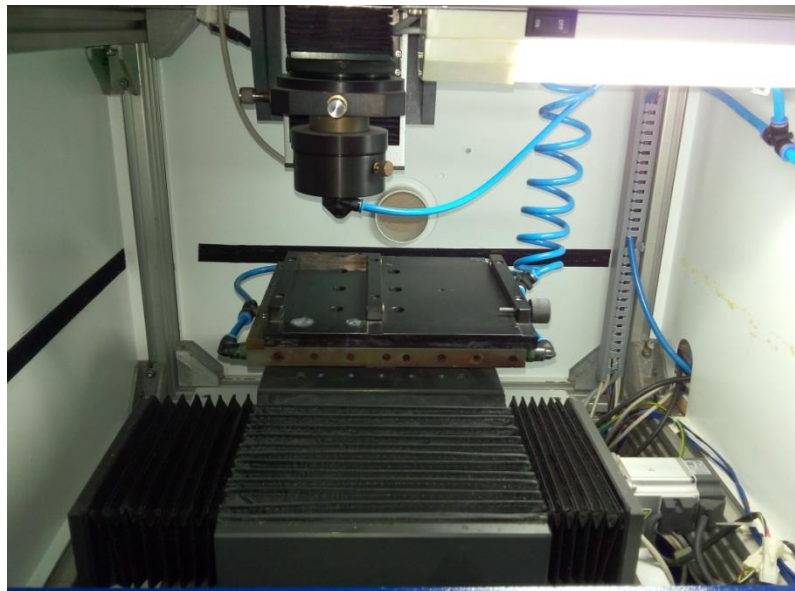

Fig: Photographic view of X-Y TABE AND Z-HEAD

Axis of travel (X-Y axis)	150mm X 150mm
Focusing vertical travel	75mm
Resolution	1µm
Table working area	150 X 150 mm^2
Clamping of Work-piece	By developed fixture
Feed rate (X, Y, & Z axis)	0.1-30 mm/s
Control system	Open Loop Control

TABLE 2: Specification of CNC table unit

CCTV and CCD camera

CCD camera gets its three-phase supply through 12V adapter. It is connected to the CCTV by a bnc cable. CCTV gets supply from single phase. A camera together with monitor is used for viewing the work piece and therefore need to align before the laser is used. The alignment consists of setting the image of the laser spot at the centre of the monitor over which a cross wire is drawn. The laser spot with lens and without lens should coincides with the centre of the cross wire.

Compressor unit

Sometimes the ablated micro chips or particles may deposited or recasted on the machining zone. To remove this impurity and clean the machining zone a compressor unit is used to suck this adhere particles. Here compressor of 2.5 Kgf/cm^2 is used.

Fig: Photographic view of Compressor Unit

Chapter-4

4. DESIGN AND DEVELOPMENT OF WORK HOLDING LASER TURNING FXTURE

Much research has been conducted on cylindrical Fibre Laser Turning System over the years. Much research works had been done in the past on parametric studies of channel cutting, drilling, welding but a very few research works carried out on turning by fibre laser set up.
To facilitate the laser micro turning operation of work piece a DC geared servo motor (150mA, 12V) is used. For micro turning a self centring rotating chuck is coupled to the RPM control unit. This set up is designed and developed easily by utilising conventional machining with the help of suitable components which includes mechanical components and electrical components. The system diagram of this fixture is depicted below
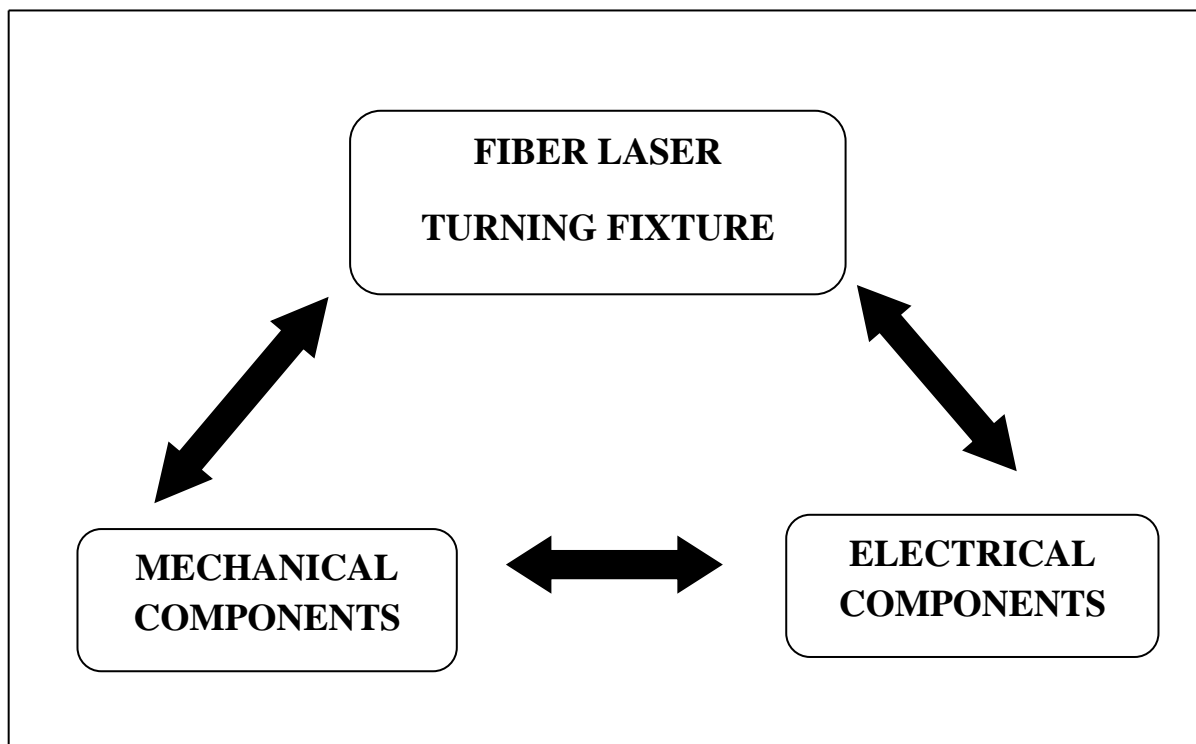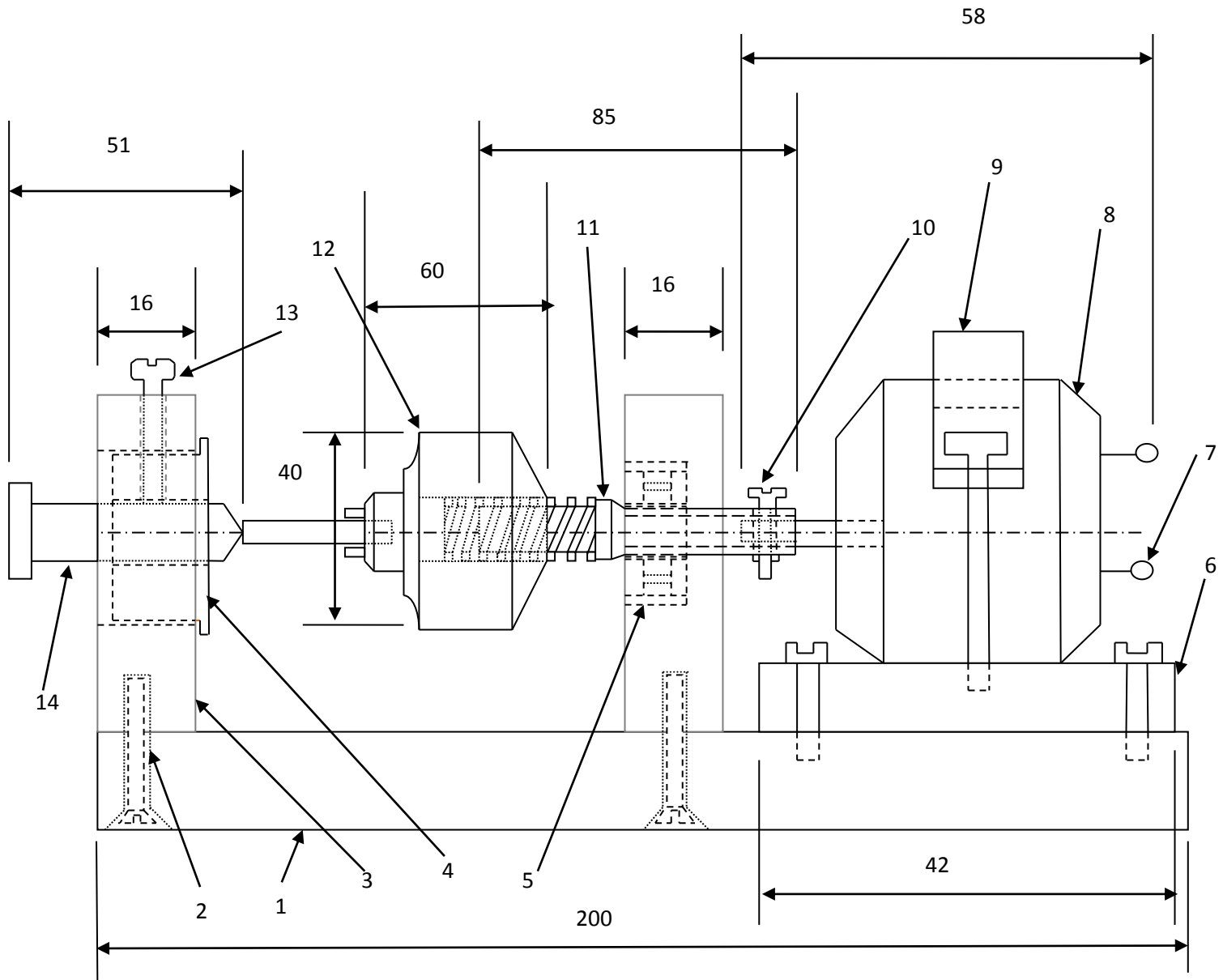
FIGURE : Block diagram Fibre Laser Turning Fixture

4.1 MAJOR REQUIREMENTS OF FIXTURE

[i] High rigidity

[ii] Minimum eccentricity of the revolution of work sample

[iii] Enhancement of RPM range

[iv] Engagement of holding micro job.

[v] Reduction of vibration.

4.2 DESIGN LAYOUT OF TURNING FIXTURE

PART NAME	PART NO	PART NAME	PART NO
BASE PLATE	1	MOTOR	8
COUNTER SUNK BOLT	2	MOTOR HOLDERS	9
EXTENDED PORTION	3	COUPLING SCREW	10
GUN METAL BUSH	4	ARBOR	11
BALL BEARING	5	HOLDING CHUCK	12
MOTOR BASE UNIT	6	LOCKING PIN	13
TERMINAL FOR POWER SUPPLY CONECTION	7	JOB-LENGTH ADJUSTABLE PIN	14

Figure: Schematic diagram of work-piece fixture
N.B: 1) All dimensions are in mm.   2) Dimensions are not to scale

4.3 MAJOR COMPONENTS OF TURNING FIXTURE

To achieve the above said requirements of work piece fixture a simple <u>TURNING SET UP</u> is indigenously made. Components of this set-up are:

1. Base plate

2. Extended Portion over plate

3. A drill chuck and its arbor

4. Alignment screws

5. Job length adjustable Pin arrangement

6. Bush for adjustable pin

7. Arbor-Ball Bearing assembly

8. Coupling of Motor shaft and Arbor by screw

9. DC geared servo motor

10. Motor- holder

11. Motor base and holder assembly

12. Motor RPM control unit

4.4 PROCEDURAL STEPS FOR DEVLOPMENT OF TURNING FIXTURE

i) Fabrication of Base Plate

For stable arrangement of work-piece fixture we need a base plate of tough and rigid material. So the base plate is made of aluminium material, it offers easy fabrication of its required dimension. According to the working area of the fibre laser CNC X-Y table the dimension of the base plate is taken. We achieve proper dimension of the base plate after shaping operation to the raw material is.

Specification of base plate :

Length = 200 mm
Width = 75 mm
Thickness = 16 mm
Material = Aluminium

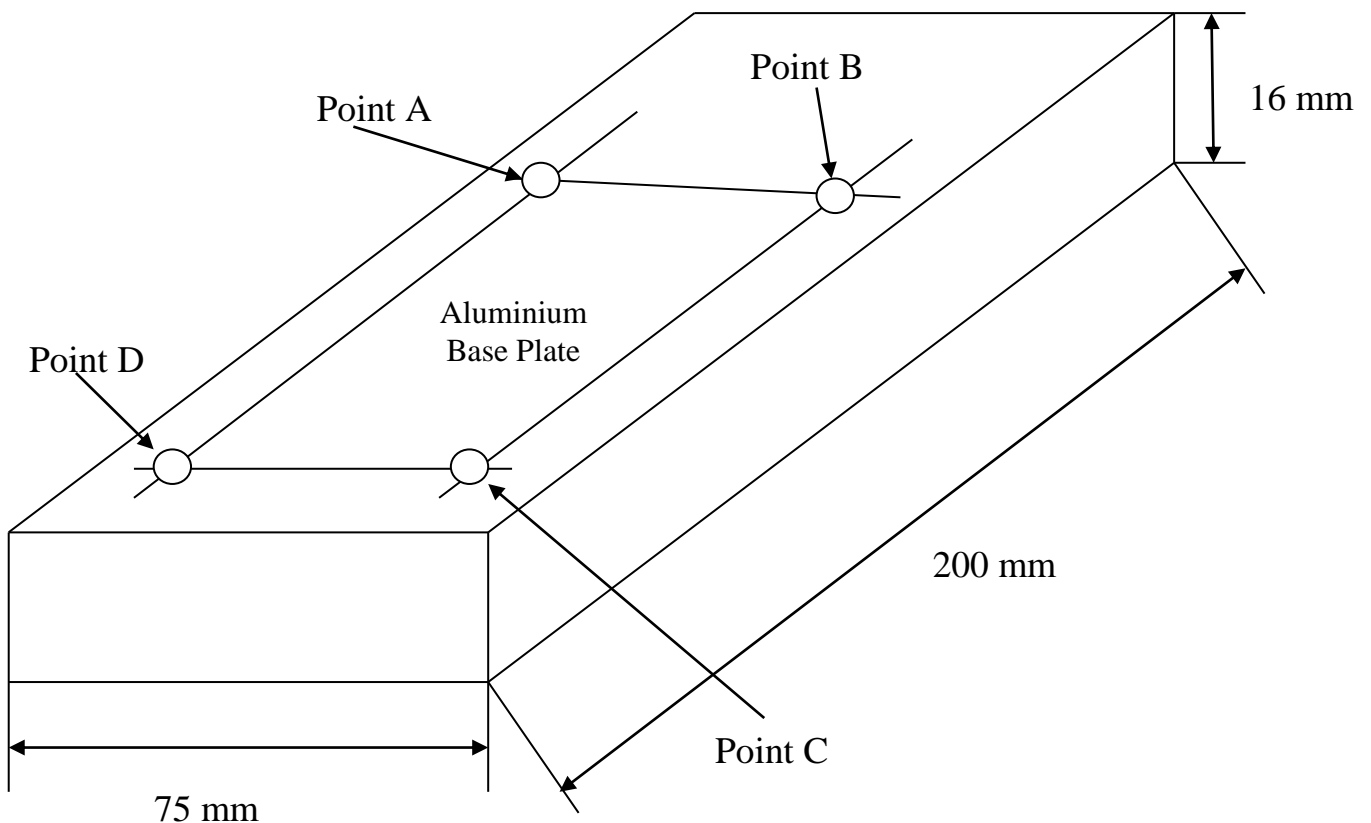The following figure1 depicted the view of base plate after machining from raw materials.

Figure 1

ii) **Fabrication of Extended portion over plate**

To hold the chuck arrangement with job two extended portion of this set up of aluminium are fabricated with equal dimensions. A drill chuck with its arbour is mounted on one of this extended part and the job length adjustable pin is mounted on another part. We get equal dimension of these extended portions after removing bars by milling operation from the surface of the raw material.

Specifications of Extended portion :

Length = 75 mm
Width = 65 mm
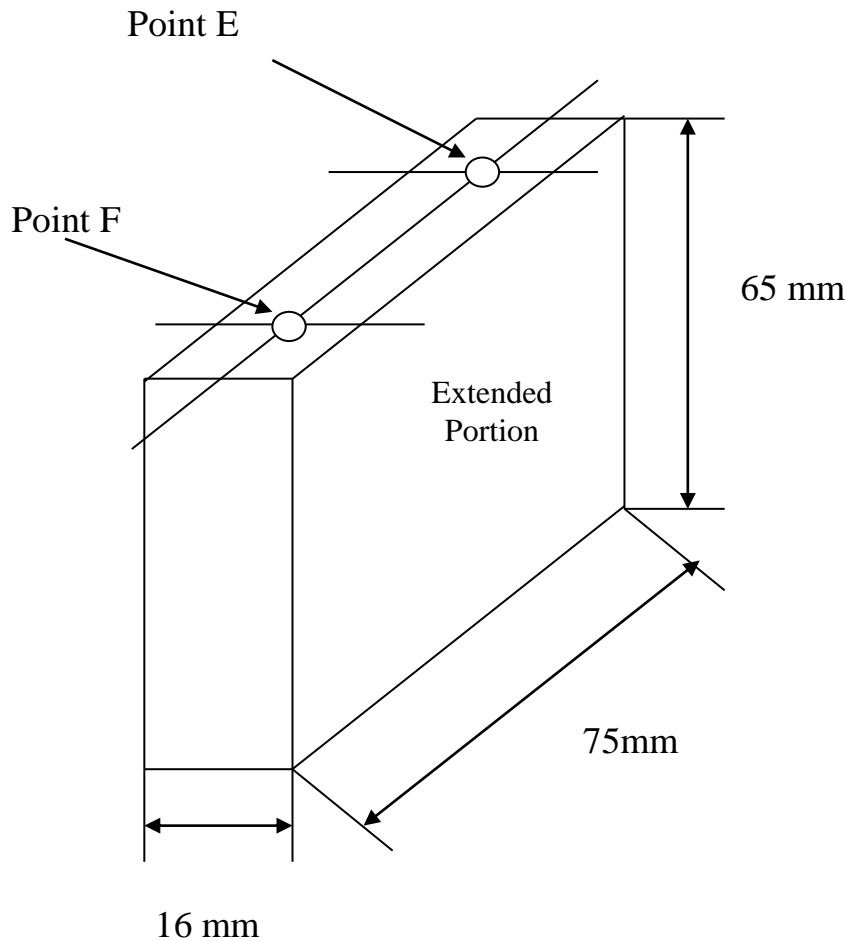Thickness = 16 mm
Material: Aluminium

Point E

Point F

65 mm

Extended
Portion

75mm

16 mm

Figure 2

iii)   Assembly of Base plate and Extended Part :

For joining these two over hanged portion ¼ inch Counter sank bolt is used. At Point A & B a through hole of diameter 6.35 mm is done though vertical drilling machine. Point E & F is projected by a Marking Indicator on the extended part. In same way the two points are projected on the other extended part. At this projected points blind drill holes of 5.1 mm are fabricated by vertical drill machine. Then a ¼ inch tap is generated in this hole through a ¼ inch tap (BSW thread) with the help of tap holding device.

The assembly of base plate and extended portions are depicted in figure3.
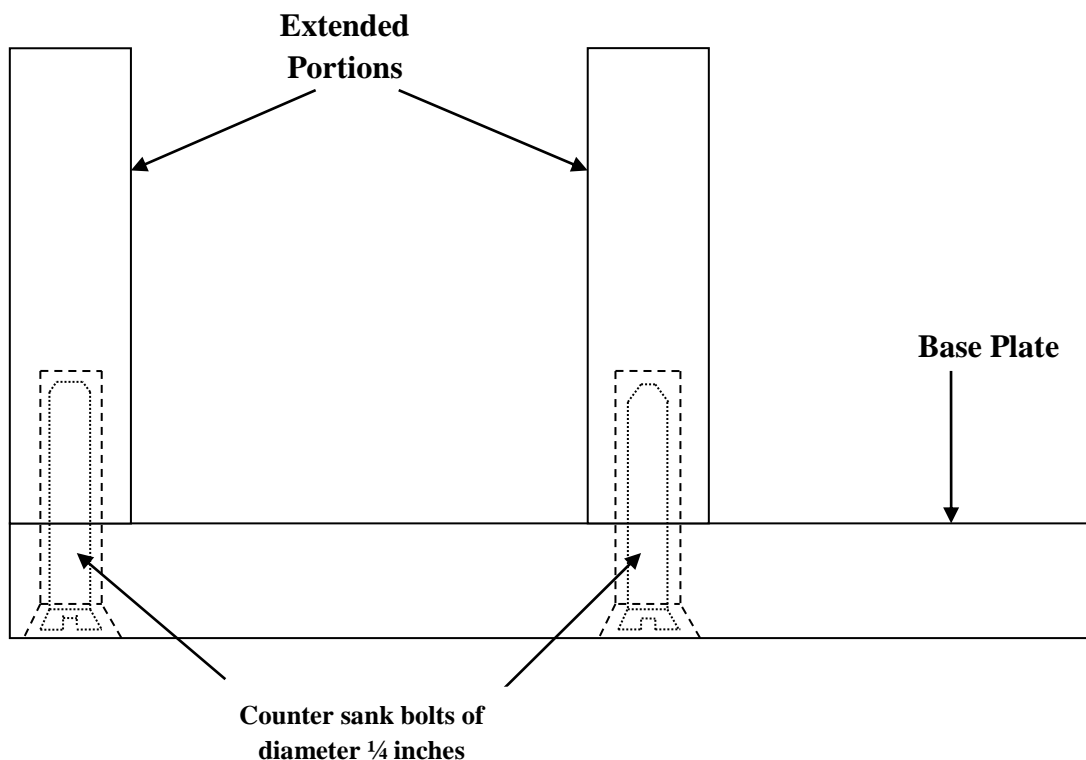

Figure 3

iv)   Drilling and Boring of the extended portion

For mounting the bush ball bearing to the left and right extended part of the plate a bore has been made. To make the two bores concentric for minimum eccentricity of the rotation of work sample the whole system is fixed in a chuck of a lathe. Then a pilot drill is operated to initialize and centring the bore. After that a ¼ inch hole is made by drill to both extended part. Then a 14 mm bore is made by lathe with a boring tool. For mounting the ball bearing a stepped bore of 3.4 mm diameter is created in right extended part with the same set up in lathe by this boring tool. Then a 25 mm bore is done on the left extended part for fixing the bush. The figure 4 shows the bore of bush and bearing.
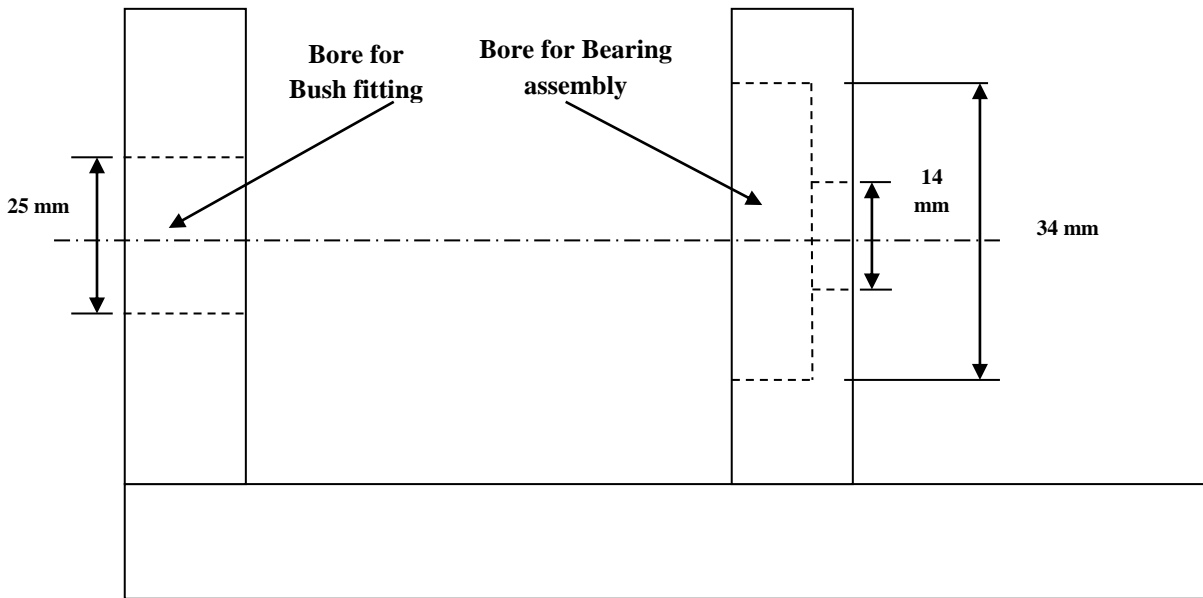
Figure 4

v) **Fitting of bush and bearing**

Bush and ball bearing are fixed to extended part by interference fit. The bush is rigidly fixed in the bore of the extended part so that the adjustable cannot move relatively to bush.

The bearing whose inner race is rotating also fitted in stepped bore so that the arbor can rotate in the bore with minimum friction. The bush is fabricated from gun metal rod. Ball bearing reduces the eccentricity of the work sample due to weight of the arbour-chuck assembly load.

Details of the Bush:

        Inner diameter d_i = 8.5 mm
        Outer diameter d_0 = 25 mm
        Material = Gun metal.

Details of Ball Bearing:

        Race Rotation = Inner race
        Outer diameter D_o = 34 mm
        Inner diameter D_i = 12.7 mm
        Bearing material = Stainless Steel
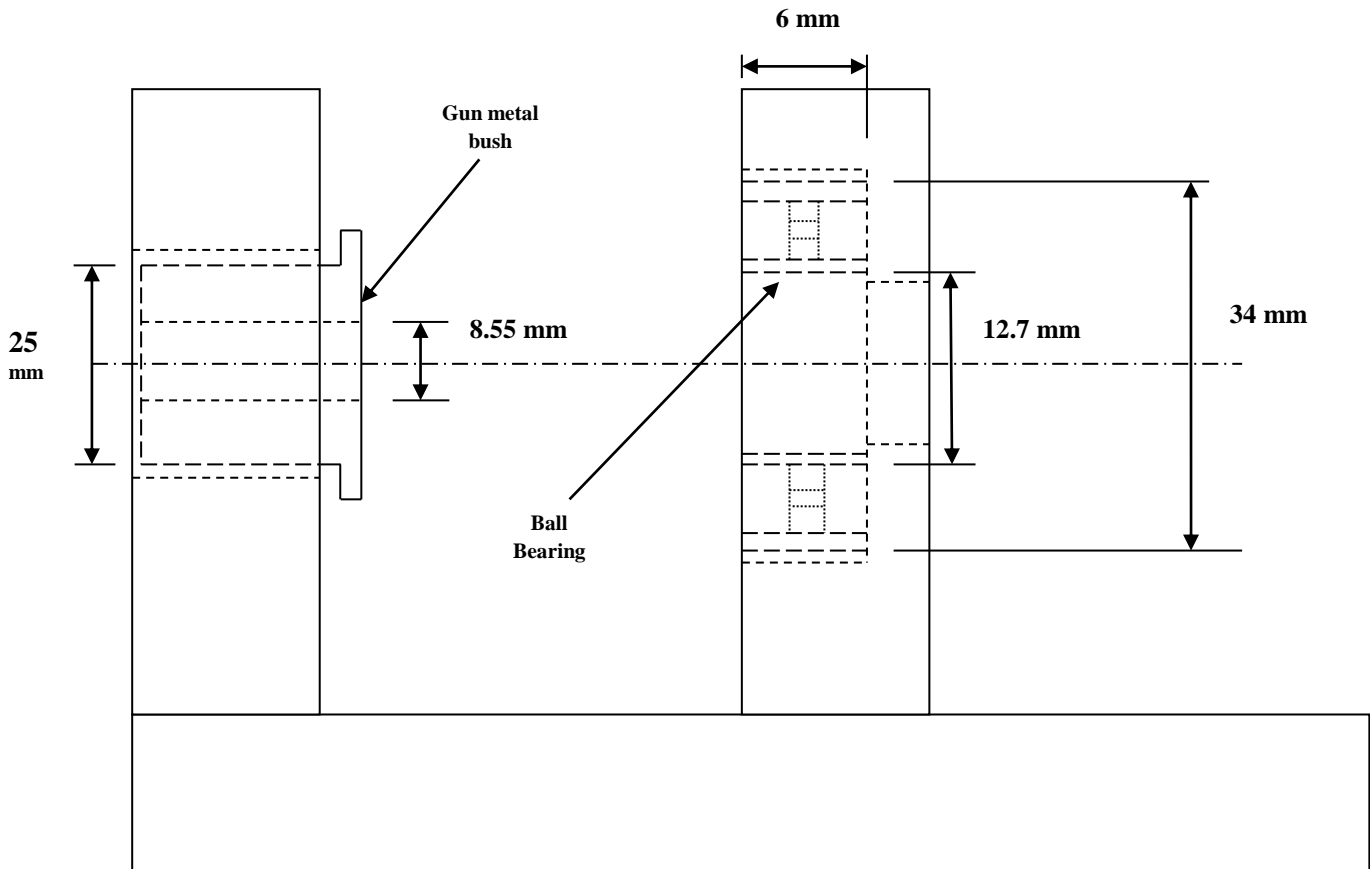
Figure 5

vi)   Arbor- chuck assembly

Arbor and job holding chuck is assembled by screw thread. The arbor is threaded at one end with flange at the middle. At the other end the arbor has annular portion to place the motor shaft in this hole.

The opening of the job holding chuck is operated by a chuck key and the other end of the chuck has internal screw thread to provide the gripping of arbor.

Job Holding Chuck Details:

Chuck Diameter = 40 mm
Chuck Length = 6 cm
Job holding capacity = 0-12 mm
Chuck material = Steel
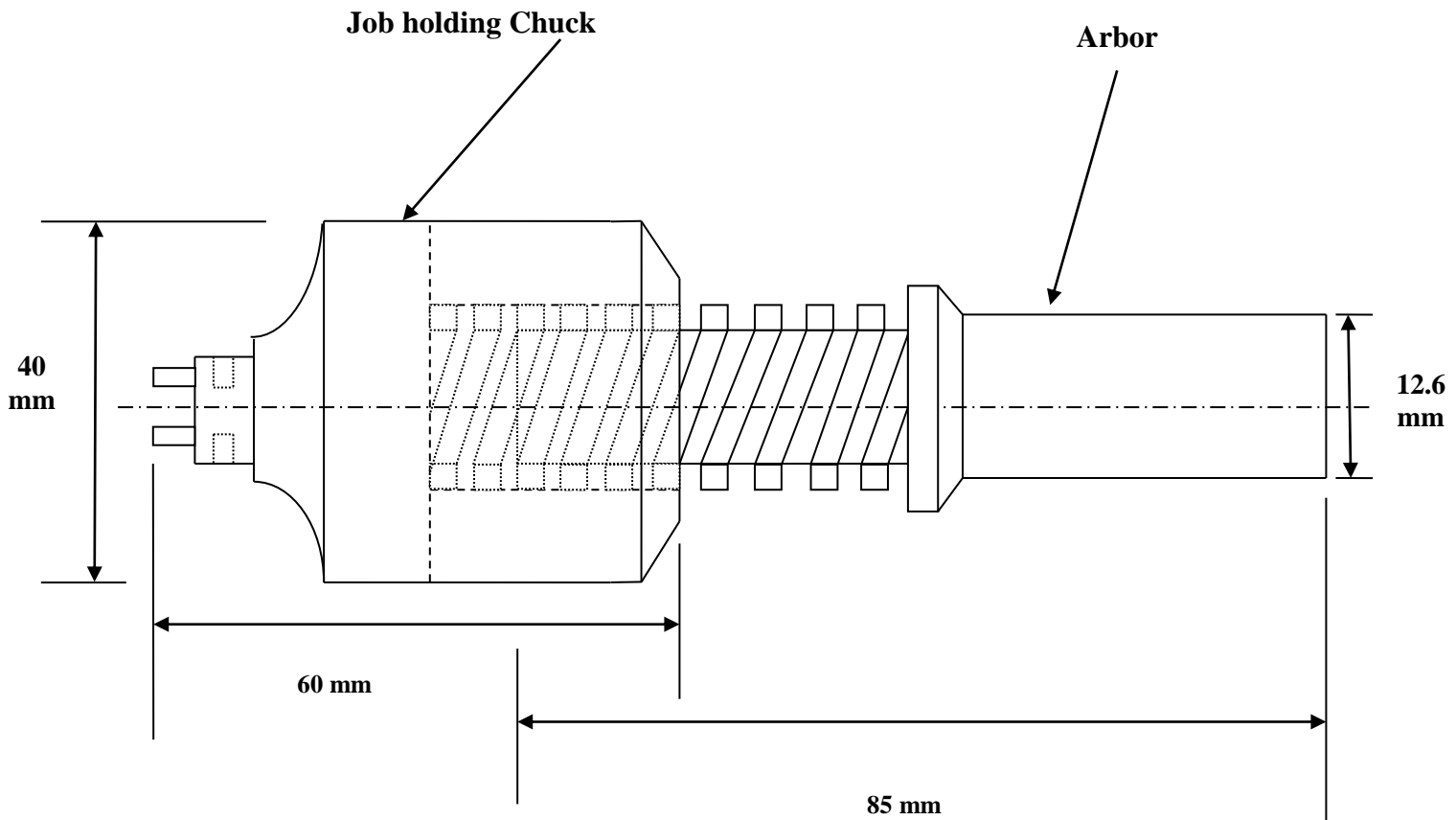
Figure 6

vii)   Coupling of Motor shaft and Arbor

In the motor shaft there is screw slot perpendicular to the axis of the motor. To mount the motor shaft with arbor a transverse hole is fabricated in the right side of the arbor piece. Then the shaft is engaged in the annular space of the arbor where the projected transverse slot is matched with the hole of the motor shaft. Then it is screwed up with a nut by screw-driver. Thus the shaft is fastened with screw and can be de-fastened again if any technical fault is occurred in motor.

Arbor Specifications:

Flange diameter = 22 mm
Coupling hole diameter = 4 mm
Thread = Metric Thread of Nominal diameter 14mm
Length span = 85 mm
Shaft outer diameter d_o = 0.5 inch
Material = Strain Hardened Cast Iron

61

viii) Motor holding arrangement

Here a DC geared motor is used for rotating the cylindrical work piece uniformly. It is linked with the abor with screw-nut assembly system. This motor is fixed on the aluminium base plate with the help of a motor base and a holder. This motor base is tightened with holder with help of screw and nut arrangement to the base plate.

DC Geared Motor:

It is a small and less spacious unit mounted on a rectangular corrugated board. It produces less noise compared to other motors. It is a very easily available and low cost unit and can operate easily.

Motor Specifications:
1. Voltage = 0-14 V DC supply
2. Max RPM = 152
3. Min RPM = 3.5
4. Shaft Diameter = 6 mm
5. Torque = 2 Kg-Cm
6. Weight = 122 gm
7. No load Current = 70 mA (max)
8. Metallic gearbox with reduction unit

The motor holder

It is an U-shaped strip which is placed on the top of the top side of the motor unit. It is made to that shape so that it restricts vibration caused during the rotation. This holder offers restriction of movement to slip the motor from its base.

Motor Holder details:
Length = 68 mm
Thickness = 2.4 mm
Width = 23 mm
Material = Aluminium

Motor Base Unit

Motor Base unit is used for levelling the motor to an exact height and to rigidly support the base of the motor, it is an rectangular strip which is fixed on the base plate with help of a screw.

Motor Base Unit Details:

Length = 42 mm
Width = 24.6 mm
Thickness = 3.2 mm
Assembly System = Screw-Nut
Material = Corrugated Board

These two parts Motor holder and Base unit are screwed by ¼ inch hexagonal screw and nut with the base plate. The figure is depicted below.

Figure 7

ix)   Fabrication of Job-length adjustable pin

For minimum eccentric rotation of the job the job-length adjustable pin support is manufactured according to the dimension of the bore created in the gun metal bush. This pin is fixed by a locking screw which is mounted on the top of the left extended part of the base. By this locking screw and pin arrangement we can easily vary the length of the job.

Details of Adjustable-Pin support:
Diameter of the Pin = 8 mm
Length of the Pin = 51 mm
Material = Steel
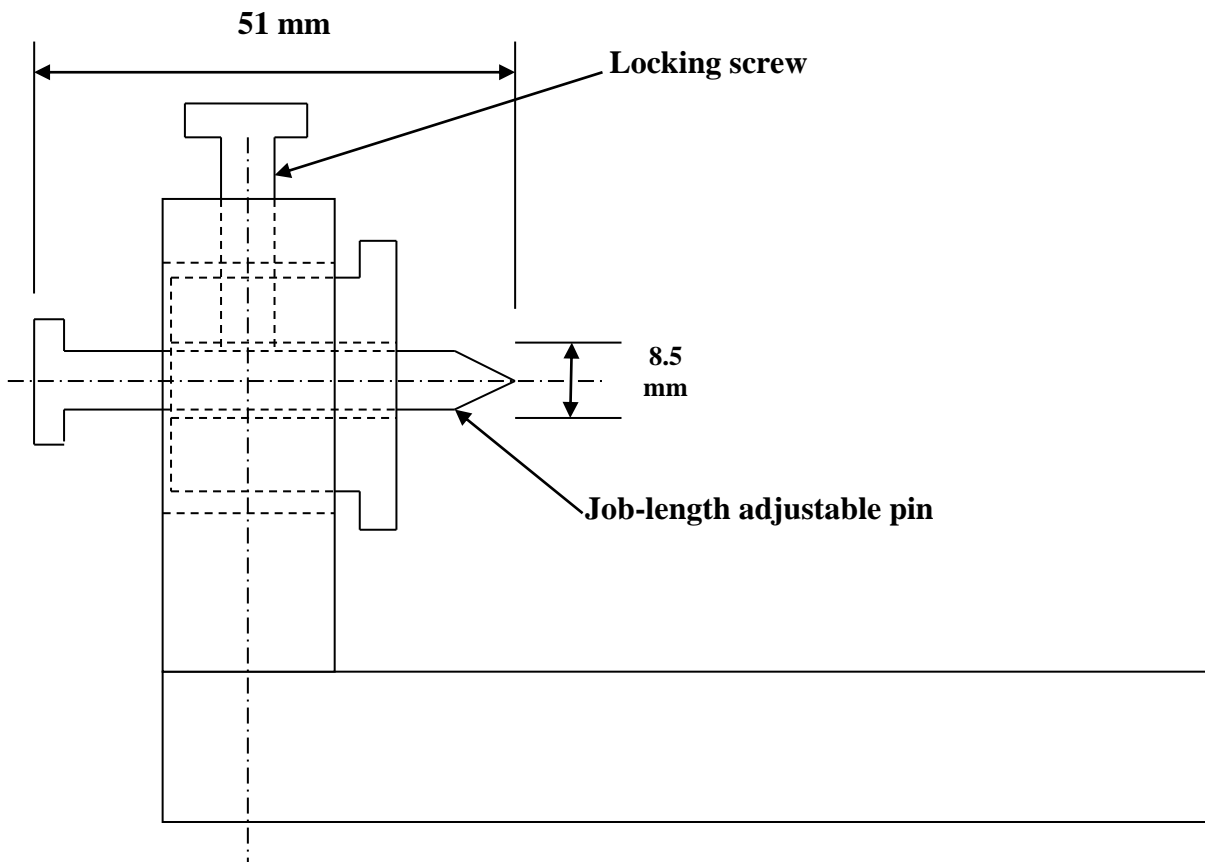
Figure 8

4.5 ROTATIONAL SPEED CONTROL UNIT

A power supply unit in conjunction with the microprocessor based voltage control unit is attached to the motor. LM2596 Buck step down Power converter Module DC 1.3-37 V digital LED voltmeter is used to precisely control the input voltage to the motor.

By controlling the voltage by this digital voltmeter (4-15V) we can vary the rotational speed of the motor upto 150 RPM.
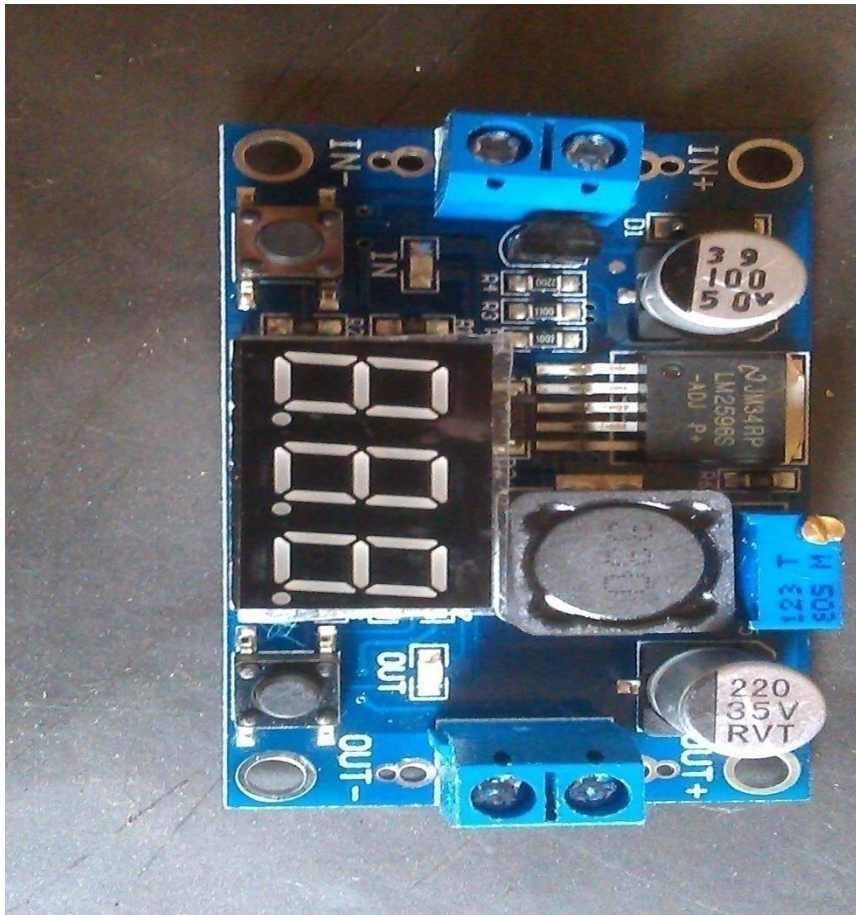
Figure : Step down digital voltmeter

4.6 ACTUAL VIEW OF DEVELOPED FIXTURE:

Accuracy:

Though all the parts are fabricated carefully and with precision the work piece is statically eccentric about 34-40μm.
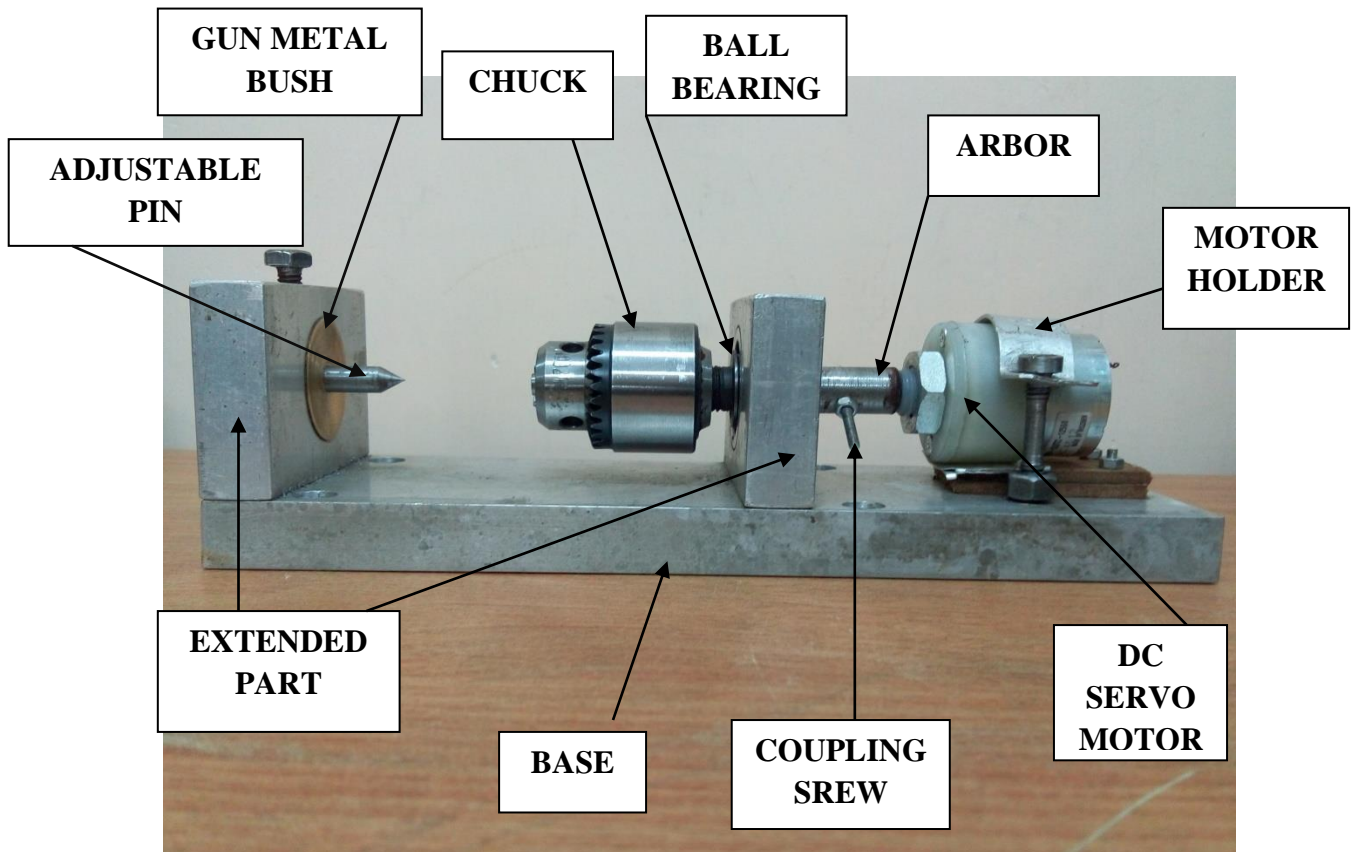
Fig: Photographic view of Work Holding Device

Solution for eccentricity and alignment problem: To remove alignment problem of the set up four threaded holes are fabricated where bolt and nut can be mounted to level the whole set-up for accurate focusing of the job surface. Here the figure is shown for aligning the job to accurate height.

Figure: Alignment bolt fixed to base plate

Chapter-5

5. EXPRIMENTAL WORK

5.1 EXPERIMENTAL SET UP

Multi diode pumped fibre laser system has been used in this work. The specifications of this laser machine are mentioned in the table given below:
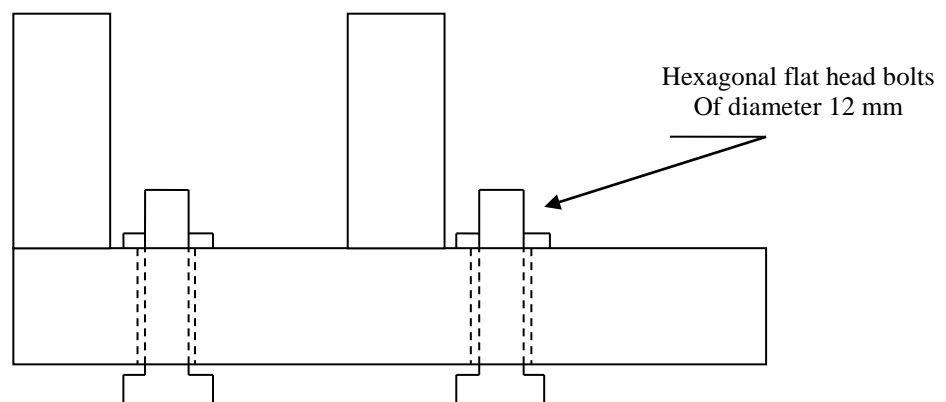
Specification	Description
Laser type	Diode Pumped Fibre Laser
Wave length	1064 nm
Mode of operation	Pulsed mode
Mode of laser beam	Fundamental/Gaussian mode (TEM_{00})
Beam diameter $1/e^2$	9 mm
Laser beam spot diameter	21 μm
Average power	7.5 KW
Pulse width	30 %

5.2 WORK-PIECE MATERIAL

In the present experimental study micro-turning of Aluminium-1060 alloy has been carried out. Aluminium-1060 alloy is a new alloy that has already performed well in various fields such as laboratory tests, in the manufacture of chemical equipment and railroad tank cars etc. The application of this material is highly viewed in technologically advanced industries.

Chemical Composition of Wrought Aluminium-1060 alloy (% weight):

Al	Si	Fe	Cu	Mn	Mg	Cr	Zn	V	Ti	Bi	Ga	Pb	Zr
99.6	0.25	0.35	0.05	0.03	0.03	0.03	0.05	0.05	0.03	0.03	0.03	0.03	0.3

In the room temperature physical properties of the alloy in its primary annealed condition are mentioned in the table:

Density (lb / cu. in.)	0.0975
Specific Gravity	2.705
Melting Point (Deg F)	1200
Modulus of Elasticity Tension	10
Modulus of Elasticity Torsion	3.85

Despite its remarkable properties, it is a considerable challenge to process the material using conventional machining due to its extreme brittleness and low fracture toughness at room temperature. Different aspects of the machining of this alloy have been investigated by several researchers. In the present work laser beam turning is studied.

5.3 EXPERIMENTAL PLAN

Taguchi's Approach to Parameter Design:

Taguchi's approach provides the designer with a systematic and efficient approach for conducting experimentation to determine near optimum settings of design parameters for performance and cost. The method emphasizes passing quality back to the design stage, seeking to design a product/process, which is insensitive to quality problems. The Taguchi method utilizes orthogonal arrays to study a large number of variables with a small number of experiments. Using orthogonal arrays significantly reduces the number of experimental configuration to be studied. The conclusion drawn from small-scale experiments are valid over the entire experimental design spanned by the control factors and their settings. This method can reduce research and developmental cost by simultaneously studying a large number of parameters.

In order to analyze the results, the Taguchi method uses a statistical measure of performance called signal-to-noise (S/N) ratio. The S/N ratio takes both the mean and the variability into account. The S/N equation depends on the criterion for the quality characteristics to be optimized. After performing the statistical analysis of S/N ratio, an analysis of variance (ANOVA) needs to be employed for estimating error variance and for determining the relative importance of various factors. In the signal-to-noise (S/N) ratio, signal refers to real value which is desired and noise refers to undesired factors in measured values. There are three basic categories to determine the best results of experiments: smaller the better characteristics, larger the better characteristics and nominal the best. The formulas are given below:

(a) Smaller the better characteristics:

$$\eta = -10 \log \left[\frac{1}{n} \sum_{i=1}^{n} y_i^2 \right]$$

(b) Larger the better characteristics:

$$\eta = -10 \log \left[\frac{1}{n} \sum_{i=1}^{n} 1/y_i^2 \right]$$

(c) Nominal the best characteristics:

$$\eta = -10 \log \left[\frac{1}{n} \sum_{i=1}^{n} (y_i - m)^{\wedge}2 \right]$$

Where y_i is measured characteristic from experiments, n is number of experiments and m is nominal value.

Orthogonal arrays offer many benefits. First, the conclusion arrive from such experiments are valid over the entire experimental region by the control factor and their settings. Second, there is a large saving in the experimental effort. Third, the data analysis is very easy.

The methodology of Taguchi for four factors at three levels is used for the implementation of the plan of orthogonal array experiments. An L9 orthogonal array with four columns and nine rows is employed in this work. The experiments are carried out according to the arrangement of the orthogonal array given in table presented later. Based upon previous literature survey and some preliminary experimentation Y-Feed Rate, Pulse Frequency, Work piece RPM, and Average Beam Power has been considered as process variables as shown in table.

Symbol	Process Parameter	Levels		
		1	2	3
X1	Y-Feed Rate (mm/s)	0.01	0.02	0.03
X2	Pulse Frequency (KHz)	60	70	80
X3	Average Beam Power (W)	70	80	90
X4	Work piece Rotational Speed (RPM)	96	118	140

TABLE: Input Factors and their Levels

Aluminium-1060 alloy rod of 4 mm diameter is used as work piece material. The material is turned to a depth in a single pass as different parametric settings as per experimental model. Air was used as assist gas in the experiments. Each experiment is performed three times and average value of the responses (Surface Roughness, Ra) is computed for each set of parameters.

Measurement of response parameter:

After completion of experiments Surface Roughness (R_a) of the round work samples are measured at four different sections with the help of MITUTOYO Surface Roughness tester.

Fig: Photographic view of Mitutoyo Surface Roughness Tester

After measuring the surface roughness at each sections average value of this data is taken.

Construction of orthogonal array:

Minitab (version 17) software has been used to create Taguchi design. The observed data from the set of experiments have been used as inputs to the software to establish mathematical models and analysis.

Experiment No.	Y-Feed Rate (mm/s)	Pulse Frequency (KHz)	Average Beam Power (W)	Workpiece Rotational Speed(RPM)
1	1	1	1	1
2	1	2	2	2
3	1	3	3	3
4	2	1	2	3
5	2	2	3	1
6	2	3	1	2
7	3	1	3	2
8	3	2	1	3
9	3	3	2	1

TABLE: L_9 Orthogonal Array (in coded form) of Taguchi Method

Chapter-6

6. ANALYSIS AND DISCUSSION OF EXPERIMENTAL RESULTS

6.1 EXPERIMENTAL RESULTS

After successful completion of the experiments the results are tabulated in the following table Main response is Surface roughness (Ra).

Exp No.	Y-Feed Rate (mm/s)	Pulse Frequency (KHz)	Average Beam Power (W)	Workpiece Rotational Speed (RPM)	Surface Roughness, Ra (µm)
1	0.1	60	70	96	3.195
2	0.1	70	80	118	2.710
3	0.1	80	90	140	2.568
4	0.2	60	80	140	2.842
5	0.2	70	90	96	2.901
6	0.2	80	70	118	3.084
7	0.3	60	90	118	3.361
8	0.3	70	70	140	3.507
9	0.3	80	80	96	4.115

TABLE: Responses of L_9 experiments.

As the present experiment is designed according to Taguchi's methodology, the Signal to Noise ratios (S/N ratio) is very important. S/N ratios of Surface roughness (Ra) of each observed values are tabulated in the following table.

Experiment No	η (Surface Roughness)
1	-10.089
2	-8.659
3	-8.191
4	-9.072
5	-9.250
6	-9.782
7	-10.529
8	-10.899
9	-12.287

TABLE: Signal to Noise (S/N) ratio values.

The signal to noise (S/N) ratio values of Surface roughness are considered as "smaller the better type".

6.2 EFFECT OF PROCESS PARAMETERS ON RESPONSE

The SN ratio plots of surface roughness with respect to Y-feed rate, pulse frequency, laser average beam power, and work piece rotational speed is shown in the following figure:
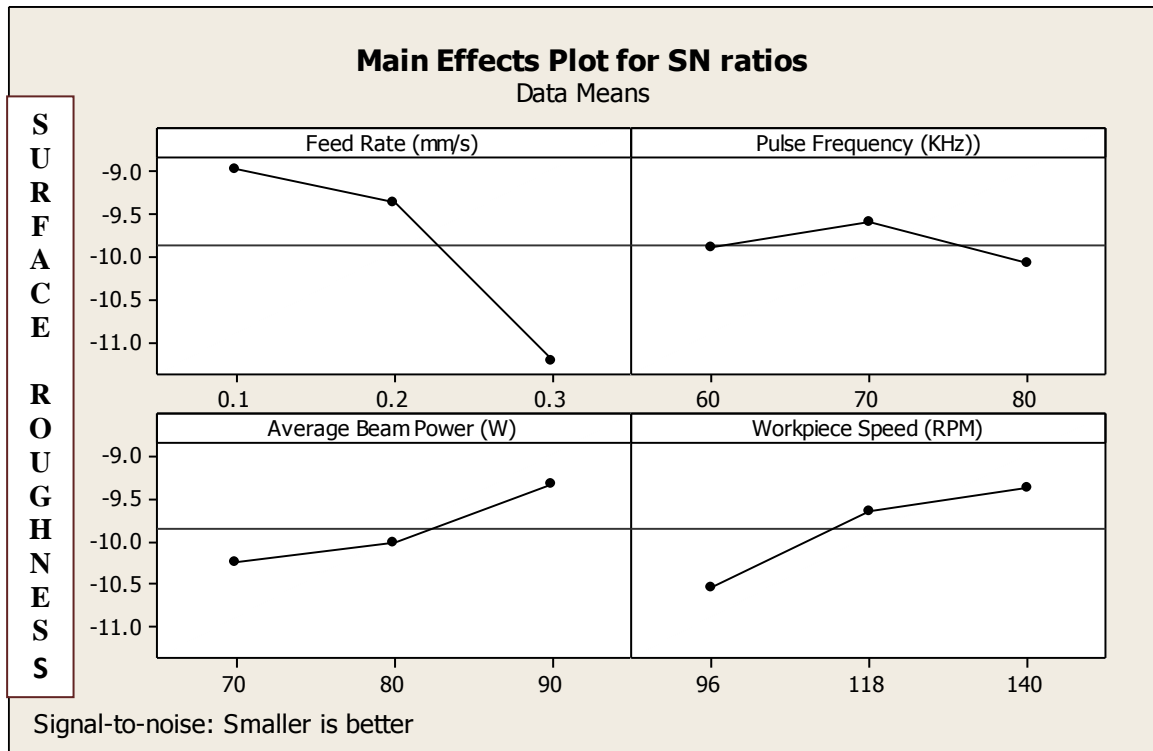

Figure: Effect of the parameters on surface roughness

Discussions:

It is observed that Surface roughness value (Ra) increases with increase in feed rate (mm/s). It is because of the fact that with increase in feed rates the circumferential overlap decreases and such the roughness value (Ra) decreases.

It is also observed that with increase in average beam power (W) and pulse frequency (KHz) Surface Roughness (Ra) value decreases. This can be explained by the fact that with increase in average beam power and pulse frequency heat flux increases which in turn in increases the radius of the machined groove and with the increase in radius surface tends to become more flat and as such roughness (Ra) value reduces.

It is noticed that surface roughness value (Ra) is not effectively dependent on pulse frequency (KHz). But overall we can reveal that surface roughness is decreases with increase in frequency because the circumferential overlap is increases.

Optimal Parametric Condition for best surface finish:
        Y-Feed Rate = 0.1 mm/s
        Pulse Frequency = 70 KHz
        Average Beam Power = 90 W
        Work piece Rotational Speed = 140 RPM

75

6.3 ANALYSIS OF VARIANCE (ANOVA) TEST

To determine the relative significance and importance of the machining process parameters considered during experimentation, the analysis of variance (ANOVA) test has been performed for the responses – surface roughness

ANOVA for surface roughness

Sources of variation	Average η (Surface Roughness) by factor level (dB)			df	Sum of Squares	Mean of Squares	Percentage Contribution
	1	2	3				
Y-Feed Rate	-8.980	-9.368	-11.233	2	8.704	4.037	63.91
Pulse Frequency	-9.897	-9.596	-10.087	2	0.490	0.245	3.87
Average Laser Beam Power	-10.25	-10.05	-9.323	2	2.396	1.198	37.94
Workpiece Rotational Speed	-10.54	-9.657	-9.882	2	1.289	0.644	10.49
Error				4	0.769	0.192	3.04
Total				12	13.018	6.316	

TABLE: ANOVA for surface roughness

Table shows the ANOVA results of surface roughness (Ra). At 95% confidence level it is revealed that Y-Feed Rate and Laser Beam Average Power affects surface roughness significantly i.e. almost 63.91% and 37.94% respectively. The other two parameters – Pulse Frequency and Work piece Rotational Speed have less effect on roughness.

Parametric Effect on Surface Roughness

ROTATIONAL SPEED (10.49%)

LASER BEAM AVERAGE POWER (37.94%)

PULSE FREQUENCY (5.96%)

Y-FEED RATE (63.91%)
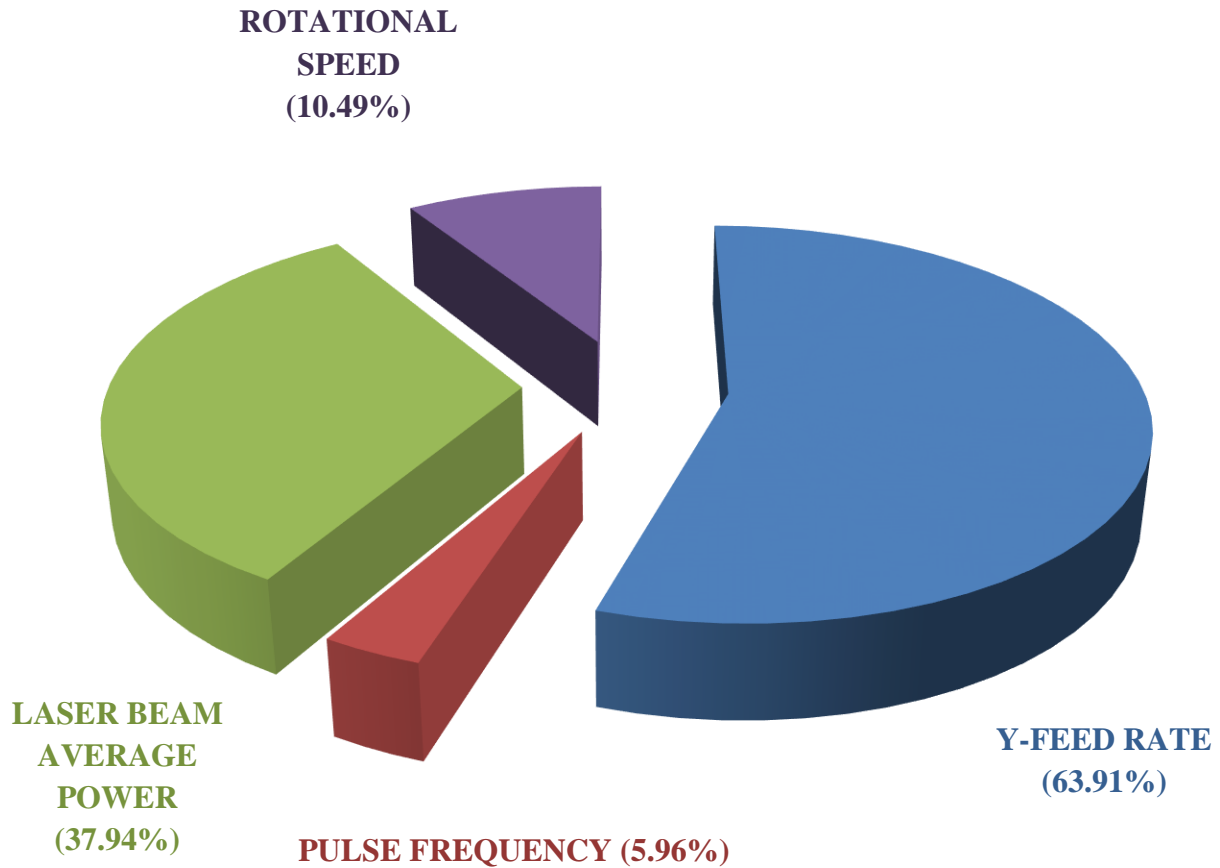
Verification Experiment at optimal parametric combinations:

Response Parameter	Predicted value at optimal setting		Experimental value at optimal setting		% of Error in S/N Ratio
	Response value	S/N Ratio	Response value	S/N Ratio	
Surface Roughness (Ra)	2.694	-8.607	2.861	-9.130	6.07

It is seen that at optimal parametric setting only 6.07% of error in S/N ratio is occurred between the predicted and experimental value of response parameter.

6.4 SUMMARY AND GENERAL CONCLUSION

In the present study an attempt has been made to investigate the capability of laser micro turning operation through in-house designed and developed set-up. Using developed set up an experimental investigation has been carried out based on Taguchi methodology. Fibre Laser micro turning process parameters such as feed rate, pulse frequency, beam power, work piece rotational speed are varied to study the effects on surface roughness. On the basis experimental results achieved the following conclusion can be made:

(a) In this research study a Fibre Laser Turning set-up has been designed and developed in order to explore the feasibility of applying cylindrical laser turning process. Using the developed set up single and multi pass turning are carried out.

(b) Based upon the experimental investigation, it is observed that Y-axis feed rate and laser beam average power play a very crucial role and they are the most significant contributing parameters for variation of surface roughness (Ra) of turned component and percentage contribution of feed rate and average beam power are 63.91 and 37.94% respectively. However other parameters like pulse frequency and rotational speed of work piece are having less significant effects on surface roughness.

(c) It is observed that surface roughness (Ra) value increases with feed rate (mm/s) and decreases with rotational speed (RPM) of work piece because the circumferential overlap decrease and increase with feed rate and rotational speed respectively.

(d) It can be clearly concluded that with increase in average beam power (W) and pulse frequency (KHz), heat flux increases which in turn increases the radius of the machined groove and with this increase in radius, surface tends to become more flat and as such roughness reduces.

(e) From the experimental investigations it is observed that optimal parametric combination is Y-Feed Rate = 0.1 mm/s, Pulse Frequency = 70 KHz, Average Beam Power = 90 W, Work piece Rotational Speed = 140 RPM for the best achievable surface finish. However, it appears that there is a further scope to enhance the surface finish by increasing the range of process parameters.

(f) To validate the proposed optimal parametric combinations, verification experiment was carried out. It was observed that the predicted optimum value is very close to the experimental result. Hence it can be concluded that Taguchi method based additive model is quite suitable tool for analysing the laser turning operation.

The present study will be useful as technological guidelines to further research in the area of laser turning operation of aluminium-1060 alloy.

There are still many areas for future research in field of laser turning. They are as follows:

(a) It can be extended for other ceramics like silicon carbide (SiC), magnesium oxide (MgO), HSTR alloys(Gamma titanium aluminide), Glass reinforced polymers etc. for industrial applications.

(b) Multi objective optimization of different process parameters under different machining condition can be carried out.

(c) There is a scope to generate intricate shapes and profiles by using laser turning operation.

Chapter-7

7. BIBILOGRAPHY

[1] Response surface method based optimization of ytterbium fiber laser parameter during machining of Al/Al2O3-MMC (31 May 2012)

[2] Process optimization of Ti–Nb alloy coatings on a Ti–6Al–4V plate using a fiber laser and blended elemental powders (26 July 2010)

[3] Machining parameter optimization of C/SiC composites using high power picosecond laser (5 January 2015)

[4] 10th International Conference on Mechanical Engineering, ICME 2013 :Modelling of Ytterbium Fiber Laser parameters during micro machining of Al-15 wt%Al2O3-MMC

[5] Optimization of deep penetration laser welding of thick stainless steel with a 10 kW fiber laser

[6] Dressing and truing of hybrid bonded CBN grinding tools using a short-pulsed fibre laser

[7] Hybrid fiber laser – Arc welding of thick section high strength low alloy steel (24 February 2011)

[8] Fibre laser cutting of thin section mild steel: An explanation of the 'striation free' effect (20 April 2011)

[9] Lasers in Manufacturing Conference 2013 : Autogeneous laser and hybrid laser arc welding of T-joint low alloy steel with fiber laser systems

[10] Fiber laser cutting of Ti6Al4V sheets for subsequent welding operations: Effect of cutting parameters on butt joints mechanical properties and strain behaviour (6 December 2012)

[11] A comparative study on fiber laser and CO2 laser welding of Inconel 617 (19 March 2015)

[12] Influence of laser power on microstructure and mechanical properties of fiber laser-tungsten inert gas hybrid welded Mg/Cu dissimilar joints (13 April 2015)

[13] Hybrid welding with fiber laser and CO2gas shielded arc (4 February 2015)

[14] Rapid micro hole laser drilling in ceramic substrates using single mode fiber laser (7 February 2015)

[15] Influence of laser scanning conditions on CFRP processing with a pulsed fiber laser (28 February 2015)

[16] Blind micro-hole array Ti6Al4V templates for carrying biomaterials fabricated by fiber laser drilling (15 March 2015)

[17] Investigation of superfast deposition of metal oxide and Diamond-Like Carbon thin films by nanosecond Ytterbium (Yb+) fiber laser (14 June 2013)

[18] LiM 2011 : Additive Generation of Surface Microstructures for Fluid-Dynamic Applications by using Single-Mode Fibre Laser Assisted Micro cladding

[19] Lasers in Manufacturing Conference 2013 : Fibre laser texturing for surface fictionalization

[20] Lasers in Manufacturing Conference 2013 : Experimental investigations on fusion cutting stainless steel with fiber and CO2 laser beams

[21] Dynamic characteristics of a multi-wavelength Brillouin–Raman fiber laser assisted by multiple four-wave mixing processes in a ring cavity (17 August 2014)

[22] Effect of glass fiber and crystallinity on light transmission during laser transmission welding of thermoplastics (21 December 2014)

[23] 978nm1.24psultra-shortplusedlargemodeareaphotoniccrystal fiber laser (28 April 2015)

[24] Tunable fiber laser using fiber Bragg gratings integrated carbon fiber composite with large tuning range (23 May 2014)

[25] Threshold characteristics analysis of a uniformly side-pumped Yb^{3+}-doped gain-guided and index-anti guided fiber laser (24 October 2014)

[26] 2 mm actively Q-switched all fiber laser based on stress-induced birefringence and commercial Tm-doped silica fiber (22 January 2015)

[27] Mode-locked erbium-doped all fiber laser using few-layer graphene as a saturable absorber (9 February 2015)

[28] Heat treatment of welded joints of steel 0.3C–1Cr–1Si produced by high-power fiber lasers (4 June 2015)

[29] A fiber laser sensor for liquid level and temperature based on two taper structures and fiber Bragg grating (25 December 2014)

[30] Stimulated Brillouin scattering in Yb^{3+}-doped dual-clad fiber lasers based on the temperature-dependent model (10 July 2014)